Octet baryon magnetic moments from QCD sum rules

Lai Wang and Frank X. Lee

Physics Department, The George Washington University, Washington, D.C. 20052, USA

(Received 25 April 2008; published 11 July 2008)

A comprehensive study is made for the magnetic moments of octet baryons in the method of QCD sum rules. A complete set of QCD sum rules is derived using the external-field method and generalized interpolating fields. For each member, three sum rules are constructed from three independent tensor structures. They are analyzed in conjunction with the corresponding mass sum rules. The performance of each of the sum rules is examined using the criteria of operator product expansion convergence and ground-state dominance, along with the role of the transitions in intermediate states. Individual contributions from the u, d, and s quarks are isolated and their implications in the underlying dynamics are explored. Valid sum rules are identified and their predictions are obtained. The results are compared with experiment and previous calculations.

DOI: 10.1103/PhysRevD.78.013003 PACS numbers: 13.40.Em, 11.55.Hx, 12.38.−t, 14.20.Gk

I. INTRODUCTION

The QCD sum rule method is a nonperturbative analytic formalism firmly entrenched in QCD with minimal modeling. The field remains active judging by the 3000 and growing references to the seminal paper of Shifman, Vainshtein, and Zakharov [1] that introduced the method. The approach provides a general way of linking hadron phenomenology with the interactions of quarks and gluons via only a few parameters: the QCD vacuum condensates and susceptibilities. The studies give a unique perspective on how the properties of hadrons arise from nonperturbative interactions in the QCD vacuum and how QCD works in this context. It has been successfully applied in almost every aspect of strong-interaction physics.

Calculations of the magnetic moment were carried out soon after the method was introduced for the proton, neutron [2,3], and hyperons [4] in the external-field method. In this method, a static magnetic field is introduced that couples to the quarks and polarizes the QCD vacuum. Magnetic moments can be extracted from the linear response to this field. The results of the studies validated the external-field method as a way of probing hadron properties other than the mass, such as magnetic moments, form factors, axial charge, or isospin breakings. Later, a more systematic study was made for the magnetic moments of octet baryons [5–8]. Calculations were also carried out for decuplet baryons [9–12] and the rho meson [13]. There are other studies of magnetic moments using the light-cone QCD sum rule method [14–17] which will not be discussed here.

In this work, we carry out a comprehensive, independent calculation of the magnetic moments of the octet baryons in the external-field method. It can be considered as an update over the previous calculations [5–7] which were done more than 20 years ago. There are a number of things we do differently. First, we employ generalized interpolating fields which allow us to use the optimal mixing of interpolating fields to achieve the best match. Second, we derive a new, complete set of QCD sum rules at all three tensor structures and analyze all of them. The previous sum rules, which were mostly limited to one of the tensor structures, correspond to a special case of the mixing in our sum rules. In this way, we provide an independent check of the previous sum rules. Third, we perform a Monte Carlo analysis which has become standard nowadays. The advantage of such an analysis is explained later. Fourth, we use a different procedure to extract the magnetic moments and to treat the transition terms in the intermediate states. Our results show that these transitions simply cannot be ignored. Fifth, we isolate the individual quark contributions to the magnetic moments and discuss their implications in the underlying quark-gluon dynamics in the baryons.

The paper is organized as follows. In Sec. II, the method of QCD sum rules is introduced. Using the interpolating fields for the octet baryons, master formulas are calculated. Then both the phenomenological representation and QCD side are derived. Section III will list the sum rules we derived for the octet baryon family, followed by the analysis to extract the magnetic moments in Sec. IV. Section V summarizes the results and gives a comparison of our results with experiment and previous calculations, followed by an in-depth discussion of our findings. Our conclusions are given in Sec. VI.

II. METHOD

The starting point is the time-ordered correlation function in the QCD vacuum in the presence of a *constant* background electromagnetic field $F_{\mu\nu}$:

$$\Pi(p) = i \int d^4x e^{ip\cdot x} \langle 0|T\{\eta(x)\bar{\eta}(0)\}|0\rangle_F. \qquad (1)$$

The QCD sum rule approach is to evaluate this correlation at two different levels. On the quark level, it describes a

hadron as quarks and gluons interacting in the QCD vacuum. On the phenomenological level, it is saturated by a tower of hadronic intermediate states with the same quantum numbers. This way, a connection can be established between a description in terms of hadronic degrees of freedom and one based on the underlying quark and gluon degrees of freedom governed by QCD. Here η is the interpolating field (or hadron current) with the quantum numbers of the hadron under consideration. The subscript F means that the correlation function is to be evaluated with an electromagnetic interaction term added to the QCD Lagrangian:

$$\mathcal{L}_I = -A_\mu J^\mu, \tag{2}$$

where A_μ is the external electromagnetic potential and $J^\mu = e_q \bar{q}\gamma^\mu q$ is the quark electromagnetic current.

Since the external field can be made arbitrarily small, one can expand the correlation function

$$\Pi(p) = \Pi^{(0)}(p) + \Pi^{(1)}(p) + \cdots, \tag{3}$$

where $\Pi^{(0)}(p)$ is the correlation function in the absence of the field, and gives rise to the mass sum rules of the baryons. The magnetic moments will be extracted from the QCD sum rules obtained from the linear response function $\Pi^{(1)}(p)$.

The action of the external electromagnetic field is twofold: it couples directly to the quarks in the baryon interpolating fields, and it also polarizes the QCD vacuum. The latter can be described by introducing new parameters called vacuum susceptibilities.

The interpolating field is constructed from quark fields with the quantum number of baryon under consideration and it is not unique. We consider a linear combination of the two standard local interpolating fields. They read for the baryon octet family:

$$\begin{aligned}
\eta^p(uud) &= -2\epsilon^{abc}[(u^{aT}C\gamma_5 d^b)u^c + \beta(u^{aT}Cd^b)\gamma_5 u^c],\\
\eta^n(ddu) &= -2\epsilon^{abc}[(d^{aT}C\gamma_5 u^b)d^c + \beta(d^{aT}Cu^b)\gamma_5 d^c],\\
\eta^\Lambda(uds) &= -2\sqrt{\frac{1}{6}}\epsilon^{abc}[2(u^{aT}C\gamma_5 d^b)s^c + (u^{aT}C\gamma_5 s^b)d^c\\
&\quad - (d^{aT}C\gamma_5 s^b)u^c + \beta(2(u^{aT}Cd^b)\gamma_5 s^c\\
&\quad + (u^{aT}Cs^b)\gamma_5 d^c - (d^{aT}Cs^b)\gamma_5 u^c)],\\
\eta^{\Sigma^-}(dds) &= -2\epsilon^{abc}[(d^{aT}C\gamma_5 s^b)d^c + \beta(d^{aT}Cs^b)\gamma_5 d^c],\\
\eta^{\Sigma^0}(uds) &= -\sqrt{2}\epsilon^{abc}[(u^{aT}C\gamma_5 s^b)d^c + (d^{aT}C\gamma_5 s^b)u^c\\
&\quad + \beta((u^{aT}Cs^b)\gamma_5 d^c + (d^{aT}Cs^b)\gamma_5 u^c)],\\
\eta^{\Sigma^+}(uus) &= -2\epsilon^{abc}[(u^{aT}C\gamma_5 s^b)u^c + \beta(u^{aT}Cs^b)\gamma_5 u^c],\\
\eta^{\Xi^-}(ssd) &= -2\epsilon^{abc}[(s^{aT}C\gamma_5 d^b)s^c + \beta(s^{aT}Cd^b)\gamma_5 s^c],\\
\eta^{\Xi^0}(ssu) &= -2\epsilon^{abc}[(s^{aT}C\gamma_5 u^b)s^c + \beta(s^{aT}Cu^b)\gamma_5 s^c].
\end{aligned} \tag{4}$$

Here u and d are up-quark and down-quark field operators, C is the charge conjugation operator, the superscript T means transpose, and ϵ_{abc} makes it a color singlet. The normalization factors are chosen so that correlation functions of these interpolating fields coincide with each other under SU(3)-flavor symmetry. The real parameter β allows for the mixture of the two independent currents. The choice advocated by Ioffe [18] and often used in QCD sum rule studies corresponds to $\beta = -1$. We will take advantage of this freedom to achieve optimal matching in the sum rule analysis.

A. Phenomenological representation

We start with the structure of the two-point correlation function in the presence of the electromagnetic vertex to first order

$$\begin{aligned}
\Pi(p) = i\int d^4x e^{ipx}\langle 0|\eta(x)\\
\times\left[-i\int d^4y A_\mu(y)J^\mu(y)\right]\bar{\eta}(0)|0\rangle.
\end{aligned} \tag{5}$$

Inserting two complete sets of physical intermediate states, we restrict our attention only to the positive energy ones and write

$$\begin{aligned}
\Pi(p) &= \int d^4x d^4y \frac{d^4k'}{(2\pi)^4}\frac{d^4k}{(2\pi)^4}\sum_{N'N}\sum_{s's}\frac{-i}{k'^2 - m_{N'}^2 - i\varepsilon}\\
&\quad\times\frac{-i}{k^2 - m_N^2 - i\varepsilon}e^{ipx}A_\mu(y)\langle 0|\eta(x)|N'k's'\rangle\\
&\quad\times\langle N'k's'|J^\mu(y)|Nks\rangle\langle Nks|\bar{\eta}(0)|0\rangle.
\end{aligned} \tag{6}$$

We can use the translation invariance to express $\eta(x)$ in terms of $\eta(0)$

$$\langle 0|\eta(x)|N'k's'\rangle = \langle 0|\eta(0)|N'k's'\rangle e^{-ik'x}. \tag{7}$$

The interpolating field excites (or annihilates) the ground state as well as the excited states of the baryon from the QCD vacuum. The ability to do so is described by a phenomenological parameter λ_N (called current coupling or pole residue), defined by the overlap for the ground state

$$\langle 0|\eta(0)|Nks\rangle = \lambda_N u(k,s), \tag{8}$$

where u is the Dirac spinor.

Translation invariance on $J^\mu(y)$ gives

$$\langle N'k's'|J^\mu(y)|Nks\rangle = e^{iqy}\langle N'k's'|J^\mu(0)|Nks\rangle, \tag{9}$$

where $q = k' - k$ is the momentum transfer and $Q^2 = -q^2$.

The matrix element of the electromagnetic current has the general form

$$\langle k's'|J^\mu(0)|ks\rangle = \bar{u}(k', s')\Big[F_1(Q^2)\gamma_\mu + F_2(Q^2)i\sigma^{\mu\nu}\frac{q^\nu}{2m_N}\Big]u(k, s), \quad (10)$$

where the Dirac form factors F_1 and F_2 are related to the Sachs form factors by

$$G_E(Q^2) = F_1(Q^2) - \frac{Q^2}{(2m_N)^2}F_2(Q^2),$$
$$G_M(Q^2) = F_1(Q^2) + F_2(Q^2). \quad (11)$$

At $Q^2 = 0$, $F_1(0) = 1$, and $F_2(0) = \mu^a$ which is the anomalous magnetic moment, and $G_M(0) = F_1(0) + F_2(0) = \mu$ which is the total magnetic moment.

Writing out explicitly only the contribution of the ground-state nucleon and denoting the excited-state contribution by ESC, we have

$$\Pi(p) = -\lambda_N^2\int d^4x d^4y \frac{d^4k'}{(2\pi)^4}\frac{d^4k}{(2\pi)^4}[k'^2 - m_N^2 - i\varepsilon]^{-1}[k^2 - m_N^2 - i\varepsilon]^{-1}A_\mu(y)e^{i(p-k')x}e^{iqy}\sum_{s'}u(k', s')\bar{u}(k', s')$$
$$\times\Big[F_1(Q^2)\gamma^\mu + F_2(Q^2)i\sigma^{\mu\nu}\frac{q^\nu}{2m_N}\Big]\sum_s u(k, s)\bar{u}(k, s) + \text{ESC}. \quad (12)$$

The spin sums are of the form

$$\sum_s u(k, s)\bar{u}(k, s) = \hat{k} + m_N. \quad (13)$$

QCD sum rule calculations are most conveniently done in the fixed-point gauge. For the electromagnetic field, it is defined by $x_\mu A_\mu(x) = 0$. In this gauge, the electromagnetic potential is given by

$$A_\mu(y) = -\tfrac{1}{2}F_{\mu\nu}y^\nu. \quad (14)$$

Changing variables from k to $q = k' - k$, then $d^4k = -d^4q$, we have

$$\Pi(p) = \frac{-\lambda_N^2}{2}F_{\mu\nu}\int d^4x d^4y \frac{d^4k'}{(2\pi)^4}\frac{d^4q}{(2\pi)^4}[k'^2 - m_N^2 - i\varepsilon]^{-1}[(q - k')^2 - m_N^2 - i\varepsilon]^{-1}e^{i(p-k')x}\Big(-i\frac{\partial}{\partial q_\nu}e^{iq\cdot y}\Big)(\hat{p} + m_N)$$
$$\times\Big[F_1(Q^2)\gamma_\mu + F_2(Q^2)i\sigma^{\mu\nu}\frac{q^\nu}{2m_N}\Big](\hat{k}' - \hat{q} + m_N) + \text{ESC}. \quad (15)$$

Integrating over x, we get a delta function

$$\int d^4x \frac{1}{(2\pi)^4}e^{i(p-k')x} = \delta^4(p - k'). \quad (16)$$

Integrating $\partial/\partial q_\nu$ by parts, then doing $\int d^4y$, we can get another delta function $\delta(q)$. Since we have a $\delta(q)$, when doing $\partial/\partial q_\nu$ only terms linear in q_ν contribute. We have $F_1(Q^2)|_{q=0} = 1$, $F_2(Q^2)|_{q=0} = \mu^a = \mu - 1$, and $\partial/\partial q_\nu F_{1,2}(Q^2)|_{q=0} = 0$, so derivatives of the structure functions do not enter. Finally, we arrive at

$$\Pi(p) = \frac{i}{2}\lambda_N^2F_{\mu\nu}[p^2 - m_N^2 - i\varepsilon]^{-2}(\hat{p} + m_N)$$
$$\times\Big\{\frac{i(\mu_N - 1)}{2m_N}\sigma^{\mu\nu}(\hat{p} + m_N) + i\sigma^{\mu\nu}$$
$$- (p^\mu\gamma^\nu - p^\nu\gamma^\mu)(\hat{p} + m_N)[p^2 - m_N^2 - i\varepsilon]^{-1}\Big\}$$
$$+ \text{ESC}. \quad (17)$$

Examination of its tensor structure reveals that it has three independent combinations: $F^{\mu\nu}(\hat{p}\sigma_{\mu\nu} + \sigma_{\mu\nu}\hat{p})$, $F^{\mu\nu}i(p_\mu\gamma_\nu - p_\nu\gamma_\mu)\hat{p}$, and $F^{\mu\nu}\sigma_{\mu\nu}$. The momentum-space correlation function in the above equation can be written in terms of these three structures:

$$\Pi(p) = -\frac{1}{4}\frac{\lambda_N^2F_{\mu\nu}}{[p^2 - m_N^2 - i\varepsilon]^2}\Big\{[\sigma^{\mu\nu}]\Big(2m_N\mu_N + \frac{\mu_N - 1}{m_N}(p^2 - m_N^2)\Big) + \mu_N[\hat{p}\sigma^{\mu\nu} + \sigma^{\mu\nu}\hat{p}]$$
$$+ \frac{2(\mu_N - 1)}{m_N}[i(p^\mu\gamma^\nu - p^\nu\gamma^\mu)]\hat{p}\Big\} + \text{ESC}, \quad (18)$$

where we have used the following identities:

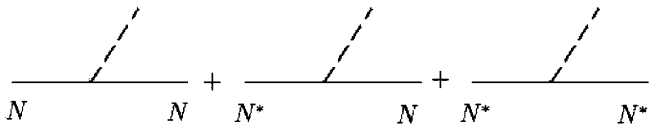

FIG. 1. The three kinds of contributions to the spectral function in the presence of an external field: ground state, transitions between ground state and excited states, and pure excited states.

$$
\begin{aligned}
&(\hat{p}+m_N)\sigma^{\mu\nu} = m_N\sigma^{\mu\nu} + \tfrac{1}{2}(\hat{p}\sigma^{\mu\nu} + \sigma^{\mu\nu}\hat{p}) + i(p^\mu\gamma^\nu - p^\nu\gamma^\mu),\\
&(\hat{p}+m_N)\sigma^{\mu\nu}(\hat{p}+m_N) = \sigma^{\mu\nu}(p^2+m_N^2) + m_N(\hat{p}\sigma^{\mu\nu} + \sigma^{\mu\nu}\hat{p}) + 2i(p^\mu\gamma^\nu - p^\nu\gamma^\mu)\hat{p},\\
&(\hat{p}+m_N)(p^\mu\gamma^\nu - p^\nu\gamma^\mu)(\hat{p}+m_N) = -(p^2-m_N^2)(p^\mu\gamma^\nu - p^\nu\gamma^\mu).
\end{aligned}
\tag{19}
$$

The next step is to perform the Borel transform defined by

$$
\hat{B}[f(p^2)] = \lim_{\substack{-p^2,n\to\infty\\ -p^2/n=M^2}} \frac{1}{n!}(-p^2)^{n+1}\left(\frac{d}{dp^2}\right)^n f(p^2). \tag{20}
$$

Upon Borel transform the ground state takes the form

$$
\begin{aligned}
\hat{B}[\Pi(p)] = &-\frac{\lambda_N^2}{4M^2}e^{-m_N^2/M^2}\Big\{\frac{1}{m_N}(2m_N^2\mu_N\\
&- M^2(\mu_N-1))[F_{\mu\nu}\sigma^{\mu\nu}]\\
&+ \mu_N[F_{\mu\nu}(\hat{p}\sigma^{\mu\nu} + \sigma^{\mu\nu}\hat{p})]\\
&+ \frac{2(\mu_N-1)}{m_N}[F_{\mu\nu}i(p^\mu\gamma^\nu - p^\nu\gamma^\mu)\hat{p}]\Big\},
\end{aligned}
\tag{21}
$$

where M is the Borel mass, not to be confused with the nucleon mass m_N.

Here we must treat the excited states with care. For a generic invariant function, the pole structure can be written as

$$
\begin{aligned}
&\frac{C_{N\leftrightarrow N}^2}{(p^2-m_N^2)^2} + \sum_{N^*}\frac{C_{N\leftrightarrow N^*}^2}{(p^2-m_N^2)(p^2-m_{N^*}^2)}\\
&+ \sum_{N^*}\frac{C_{N^*\leftrightarrow N^*}^2}{(p^2-m_{N^*}^2)^2},
\end{aligned}
\tag{22}
$$

where $C_{N\leftrightarrow N}$, $C_{N\leftrightarrow N^*}$, and $C_{N^*\leftrightarrow N^*}$ are constants. The first term is the ground-state pole which contains the desired magnetic moment μ_N. The second term represents the nondiagonal transitions between the ground state and the excited states caused by the external field. The third term is pure excited-state contributions. These different contributions can be represented by the diagrams in Fig. 1. Upon Borel transform, it takes the form

$$
\begin{aligned}
&\frac{\lambda_N^2\mu_N}{M^2}e^{-m_N^2/M^2} + e^{-m_N^2/M^2}\Big[\sum_{N^*}\frac{C_{N\leftrightarrow N^*}^2}{m_{N^*}^2-m_N^2}(1\\
&- e^{-(m_{N^*}^2-m_N^2)/M^2})\Big] + \sum_{N^*}\frac{C_{N^*\leftrightarrow N^*}^2}{M^2}e^{-m_{N^*}^2/M^2}.
\end{aligned}
\tag{23}
$$

The important point is that the transitions give rise to a contribution that is not exponentially suppressed relative to the ground state. This is a general feature of the external-field technique. The strength of such transitions at each structure is *a priori* unknown and is an additional source of contamination in the determination of the magnetic moment μ_N. The standard treatment of the transitions is to approximate the quantity in the square brackets by a constant, which is to be extracted from the sum rule along with the ground-state property of interest. Inclusion of such contributions is necessary for the correct extraction of the magnetic moments. The pure excited-state contributions are exponentially suppressed relative to the ground state and can be modeled in the usual way by introducing a continuum model and threshold parameter.

B. Calculation of the QCD side

We start by contracting out the quark pairs in Eq. (1) using Wick's theorem, resulting in the so-called *master formula* in terms of quark propagators. The master formula for the proton (with uud quark content) is

$$
\begin{aligned}
\langle\Omega|T\{\eta^N(x)\bar{\eta}^N(0)|\Omega\rangle = &-4\epsilon^{abc}\epsilon^{a'b'c'}\{S_u^{aa'}\gamma_5 C S_d^{cc'T} C\gamma_5 S_u^{bb'} + S_u^{aa'}\,\mathrm{Tr}(C S_d^{cc'T} C\gamma_5 S_u^{bb'}\gamma_5) + \beta\gamma_5 S_u^{aa'}\gamma_5 C S_d^{cc'T} C S_u^{bb'}\\
&+ \beta\gamma_5 S_u^{aa'}\,\mathrm{Tr}(C S_u^{cc'T} C S_d^{bb'}\gamma_5) + \beta S_u^{aa'} C S_d^{cc'T} C\gamma_5 S_u^{bb'}\gamma_5 + \beta S_u^{aa'}\gamma_5\,\mathrm{Tr}(C S_u^{cc'T} C\gamma_5 S_d^{bb'})\\
&+ \beta^2\gamma_5 S_u^{aa'} C S_d^{cc'T} C S_u^{bb'}\gamma_5 + \beta^2\gamma_5 S_u^{aa'}\gamma_5\,\mathrm{Tr}(C S_d^{cc'T} C S_u^{bb'})\}.
\end{aligned}
\tag{24}
$$

The master formula for the neutron (with ddu quark content) can be obtained by exchanging the d quark with a u quark from Eq. (24). By replacing the d quark with a s quark, one can get the master formula for Σ^+ (with uus quark content), while the master formula for Σ^- (with uus quark content) can be obtained by replacing the u quark with a d quark from the Σ^+ master formula. By exchanging the u quarks and s quarks in the Σ^+ master formula, the master formula for Ξ^0 (with ssu quark content) can be obtained. Likewise, by replacing the u quark with a d quark, one can get the master formula for Ξ^+ (with ssd quark content).

The master formulas for Σ^0 and Λ (uds quark content) have a more complicated structure. They can be written in a combined way as

$$\begin{aligned}\langle\Omega|T\{\eta(x)\bar{\eta}(0)\}|\Omega\rangle = & -f\epsilon^{abc}\epsilon^{a'b'c'}\{f_1 f_2 S_s^{aa'}\gamma_5 C S_u^{cc'T} C\gamma_5 S_d^{bb'} - f_1 f_3 S_s^{aa'}\gamma_5 C S_d^{cc'T} C\gamma_5 S_u^{bb'} \\ & + f_1 f_1 S_s^{aa'}\,\mathrm{Tr}(C S_u^{cc'T} C\gamma_5 S_d^{bb'}\gamma_5) + f_2 f_1 S_d^{aa'}\gamma_5 C S_u^{cc'T} C\gamma_5 S_s^{bb'} + f_2 f_3 S_d^{aa'}\gamma_5 C S_s^{cc'T} C\gamma_5 S_u^{bb'} \\ & + f_2 f_2 S_d^{aa'}\,\mathrm{Tr}(C S_s^{cc'T} C\gamma_5 S_u^{bb'}\gamma_5) - f_3 f_1 S_u^{aa'}\gamma_5 C S_d^{cc'T} C\gamma_5 S_s^{bb'} + f_3 f_2 S_u^{aa'}\gamma_5 C S_s^{cc'T} C\gamma_5 S_d^{bb'} \\ & + f_3 f_3 S_u^{aa'}\,\mathrm{Tr}(C S_s^{cc'T} C\gamma_5 S_d^{bb'}\gamma_5) + f_1 f_5\beta S_s^{aa'} C S_u^{cc'T} C\gamma_5 S_d^{bb'}\gamma_5 - f_1 f_6\beta S_s^{aa'} C S_d^{cc'T} C\gamma_5 S_u^{bb'}\gamma_5 \\ & + f_1 f_4\beta S_s^{aa'}\gamma_5\,\mathrm{Tr}(C S_d^{cc'T} C\gamma_5 S_u^{bb'}) + f_2 f_4\beta S_d^{aa'} C S_u^{cc'T} C\gamma_5 S_s^{bb'}\gamma_5 + f_2 f_6\beta S_d^{aa'} C S_s^{cc'T} C\gamma_5 S_u^{bb'}\gamma_5 \\ & + f_2 f_5\beta S_d^{aa'}\gamma_5\,\mathrm{Tr}(C S_s^{cc'T} C\gamma_5 S_u^{bb'}) - f_3 f_4\beta S_u^{aa'} C S_d^{cc'T} C\gamma_5 S_s^{bb'}\gamma_5 + f_3 f_5\beta S_u^{aa'} C S_s^{cc'T} C\gamma_5 S_d^{bb'}\gamma_5 \\ & + f_3 f_6\beta S_u^{aa'}\gamma_5\,\mathrm{Tr}(C S_s^{cc'T} C\gamma_5 S_d^{bb'}) + f_4 f_2\beta\gamma_5 S_s^{aa'}\gamma_5 C S_u^{cc'T} C S_d^{bb'} - f_4 f_3\beta\gamma_5 S_s^{aa'}\gamma_5 C S_d^{cc'T} C S_u^{bb'} \\ & + f_4 f_1\beta\gamma_5 S_s^{aa'}\,\mathrm{Tr}(C S_d^{cc'T} C S_u^{bb'}\gamma_5) + f_5 f_1\beta\gamma_5 S_d^{aa'}\gamma_5 C S_u^{cc'T} C S_s^{bb'} + f_5 f_3\beta\gamma_5 S_d^{aa'}\gamma_5 C S_s^{cc'T} C S_u^{bb'} \\ & + f_5 f_2\beta\gamma_5 S_d^{aa'}\,\mathrm{Tr}(C S_s^{cc'T} C S_u^{bb'}\gamma_5) - f_6 f_1\beta\gamma_5 S_u^{aa'}\gamma_5 C S_d^{cc'T} C S_s^{bb'} + f_6 f_2\beta\gamma_5 S_u^{aa'}\gamma_5 C S_s^{cc'T} C S_d^{bb'} \\ & + f_6 f_3\beta\gamma_5 S_u^{aa'}\,\mathrm{Tr}(C S_s^{cc'T} C S_d^{bb'}\gamma_5) + f_4 f_5\beta^2\gamma_5 S_s^{aa'} C S_u^{cc'T} C S_d^{bb'}\gamma_5 - f_4 f_6\beta^2\gamma_5 S_s^{aa'} C S_d^{cc'T} C S_u^{bb'}\gamma_5 \\ & + f_4 f_4\beta^2\gamma_5 S_s^{aa'}\gamma_5\,\mathrm{Tr}(C S_u^{cc'T} C S_d^{bb'}) + f_5 f_4\beta^2\gamma_5 S_d^{aa'} C S_u^{cc'T} C S_s^{bb'}\gamma_5 + f_5 f_6\beta^2\gamma_5 S_d^{aa'} C S_s^{cc'T} C S_u^{bb'}\gamma_5 \\ & + f_5 f_5\beta^2\gamma_5 S_d^{aa'}\gamma_5\,\mathrm{Tr}(C S_s^{cc'T} C S_u^{bb'}) - f_6 f_4\beta^2\gamma_5 S_u^{aa'} C S_d^{cc'T} C S_s^{bb'}\gamma_5 + f_6 f_5\beta^2\gamma_5 S_u^{aa'} C S_s^{cc'T} C S_d^{bb'}\gamma_5 \\ & + 4 f_6 f_6\beta^2\gamma_5 S_u^{aa'}\gamma_5\,\mathrm{Tr}(C S_s^{cc'T} C S_d^{bb'})\}, \end{aligned} \tag{25}$$

where the various factors are as follows: for Σ^0, $f = 2$, $f_1 = 0$, $f_2 = 1$, $f_3 = 1$, $f_4 = 0$, $f_5 = 1$, $f_6 = 1$; and for Λ, $f = 2/3$, $f_1 = 2$, $f_2 = 1$, $f_3 = -1$, $f_4 = 2$, $f_5 = 1$, $f_6 = -1$.

In the above equations,

$$S_q^{ab}(x, 0; F) \equiv \langle 0|T\{q^a(x)\bar{q}^b(0)\}|0\rangle_F, \qquad q = u, d, s, \tag{26}$$

is the fully interacting quark propagator in the presence of the electromagnetic field. To first order in $F_{\mu\nu}$ and m_q (assume $m_u = m_d = 0$, $m_s \neq 0$), and order x^4, it is given by the operator product expansion (OPE) [3,6,7]:

$$\begin{aligned} S_q^{ab}(x, 0; Z) \equiv & \frac{i}{2\pi^2}\frac{\hat{x}}{x^4}\delta^{ab} - \frac{m_q}{4\pi^2 x^2}\delta^{ab} - \frac{1}{12}\langle\bar{q}q\rangle\delta^{ab} + \frac{im_q}{48}\langle\bar{q}q\rangle\hat{x}\delta^{ab} + \frac{1}{192}\langle\bar{q}g_c\sigma\cdot Gq\rangle x^2\delta^{ab} \\ & - \frac{im_q}{1152}\langle\bar{q}g_c\sigma\cdot Gq\rangle\hat{x}x^2\delta^{ab} - \frac{1}{3^3 2^{10}}\langle\bar{q}q\rangle\langle g_c^2 G^2\rangle x^4\delta^{ab} + \frac{i}{32\pi^2}(g_c G^n_{\alpha\beta})\frac{\hat{x}\sigma^{\alpha\beta} + \sigma^{\alpha\beta}\hat{x}}{x^2}\left(\frac{\lambda^n}{2}\right)^{ab} \\ & + \frac{1}{48}\frac{i}{32\pi^2}\langle g_c^2 G^2\rangle\frac{\hat{x}\sigma^{\alpha\beta} + \sigma^{\alpha\beta}\hat{x}}{x^2}\left(\frac{\lambda^n}{2}\right)^{ab} + \frac{1}{3^2 2^{10}}\langle\bar{q}q\rangle\langle g_c^2 G^2\rangle x^2\sigma^{\alpha\beta}\left(\frac{\lambda^n}{2}\right)^{ab} - \frac{1}{192}\langle\bar{q}g_c\sigma\cdot Gq\rangle\sigma^{\alpha\beta}\left(\frac{\lambda^n}{2}\right)^{ab} \\ & + \frac{im_q}{768}\langle\bar{q}g_c\sigma\cdot Gq\rangle(\hat{x}\sigma^{\alpha\beta} + \sigma^{\alpha\beta}\hat{x})\left(\frac{\lambda^n}{2}\right)^{ab} + \frac{ie_q}{32\pi^2}F_{\alpha\beta}\frac{\hat{x}\sigma^{\alpha\beta} + \sigma^{\alpha\beta}\hat{x}}{x^2}\delta^{ab} - \frac{e_q}{24}\chi\langle\bar{q}q\rangle F_{\alpha\beta}\sigma^{\alpha\beta}\delta^{ab} \\ & + \frac{ie_q m_q}{96}\chi\langle\bar{q}q\rangle F_{\alpha\beta}(\hat{x}\sigma^{\alpha\beta} + \sigma^{\alpha\beta}\hat{x})\delta^{ab} + \frac{e_q}{288}\langle\bar{q}q\rangle F_{\alpha\beta}(x^2\sigma^{\alpha\beta} - 2x_\rho x^\beta\sigma^{\beta\alpha})\delta^{ab} \\ & + \frac{e_q}{576}\langle\bar{q}q\rangle F_{\alpha\beta}[x^2(\kappa + \xi)\sigma^{\alpha\beta} - x_\rho x^\beta(2\kappa - \xi)\sigma^{\beta\alpha}]\delta^{ab} - \frac{e_q}{16}\langle\bar{q}q\rangle\left(\kappa F_{\alpha\beta} - \frac{i}{4}\xi\epsilon_{\alpha\beta\mu\nu}F^{\mu\nu}\right)\left(\frac{\lambda^n}{2}\right)^{ab} \\ & + \text{ higher order terms.} \end{aligned} \tag{27}$$

We use the convention $\epsilon^{0123} = +1$ in this work.

In addition to the standard vacuum condensates, the vacuum susceptibilities induced by the external field are defined by

$$\begin{aligned} \langle\bar{q}\sigma_{\mu\nu}q\rangle_F &\equiv e_q\chi\langle\bar{q}q\rangle F_{\mu\nu}, \\ \langle\bar{q}g_c G_{\mu\nu}q\rangle_F &\equiv e_q\kappa\langle\bar{q}q\rangle F_{\mu\nu}, \\ \langle\bar{q}g_c\epsilon_{\mu\nu\rho\lambda}G^{\rho\lambda}\gamma_5 q\rangle_F &\equiv ie_q\xi\langle\bar{q}q\rangle F_{\mu\nu}. \end{aligned} \tag{28}$$

Note that χ has the dimension of GeV^{-2}, while κ and ξ are dimensionless.

With the above elements in hand, it is straightforward to evaluate the correlation function by substituting the quark propagator into the various master formulas. We keep terms to first order in the external field and in the strange quark mass. Terms up to dimension 8 are considered. The algebra is extremely tedious. Each term in the master formula is a product of three copies of the quark propagator. There are hundreds of such terms over various color

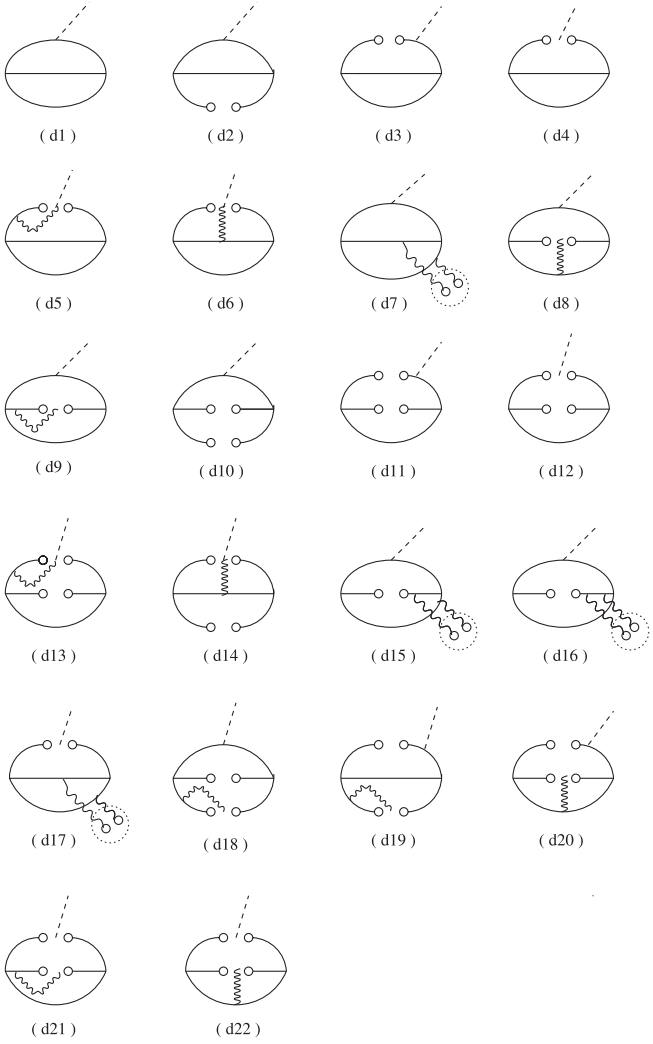

FIG. 2. Nonmass diagrams considered for the octet baryon magnetic moments.

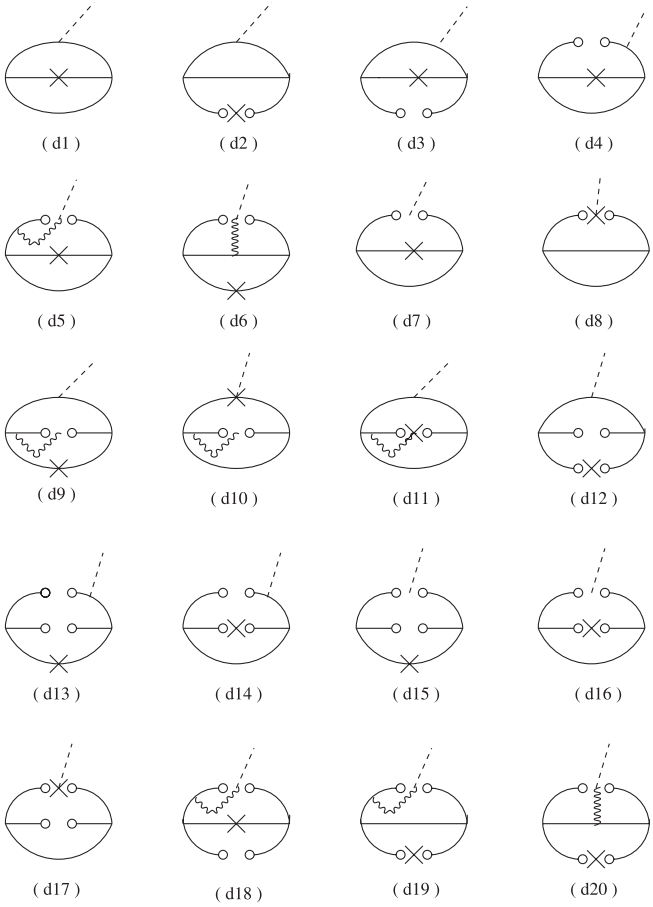

FIG. 3. Diagrams considered for the strange quark mass corrections to the octet baryon magnetic moments.

permutations. The calculation can be organized by diagrams (similar to Feynmann diagrams) in Figs. 2 and 3. Note that each diagram is only generic and all possible color permutations are understood. The QCD side has the same tensor structure as the phenomenological side and the results can be organized according to the same three independent structures.

III. QCD SUM RULES

Once we have both the QCD side [left-hand side (LHS)] and the phenomenological side [right-hand side (RHS)], we can derive the sum rules by matching both sides. Since there are three independent tensor structures, three sum rules can be constructed. We denote these tensor structures by the following shorthand notation

$$\mathrm{WE}_1 = F^{\mu\nu}(\hat{p}\sigma_{\mu\nu} + \sigma_{\mu\nu}\hat{p}), \tag{29}$$

$$\mathrm{WO}_1 = F^{\mu\nu}\sigma_{\mu\nu}, \tag{30}$$

$$\mathrm{WO}_2 = F^{\mu\nu} i(p_\mu \gamma_\nu - p_\nu \gamma_\mu)\hat{p}. \tag{31}$$

The sum rule from WE_1 involves only dimension-even condensates, so we call this sum rule chiral even. The sum rule from both WO_1 and WO_2 involves only dimension-odd condensates, so we call them chiral odd. Note that in previous works [3,5] the dimension of the tensor structures, rather than the dimension of the condensates, was used to refer to the sum rules. The two names are opposite.

Now we are ready to collect all of the QCD sum rules. At the structure WE_1, all of the sum rules can be expressed in the following form:

$$\begin{aligned} & c_1 L^{-4/9} E_2(w) M^4 + c_2 m_s \chi a L^{-26/27} E_1(w) M^2 \\ & \quad + c_3 \chi a^2 L^{-4/27} E_0(w) + c_4 b L^{-4/9} E_0(w) \\ & \quad + (c_5 + c_6) m_s a L^{-4/9} E_0(w) + (c_7 + c_8) a^2 L^{4/9} \frac{1}{M^2} \\ & \quad + c_9 \chi m_0^2 a^2 L^{-18/27} \frac{1}{M^2} + c_{10} m_s m_0^2 a L^{-26/27} \frac{1}{M^2} \\ & = -\tilde{\lambda}_N^2 \left[\frac{\mu_N}{M^2} + A \right] e^{-m_N^2/M^2}, \end{aligned} \tag{32}$$

where the coefficients differ from member to member, and the current coupling is rescaled as $\tilde{\lambda}_N^2 \equiv (2\pi)^4 \lambda_N^2$ to remove factors of π in the sum rule. The quark condensate, gluon condensate, and the mixed condensate are

$$a = -(2\pi)^2\langle\bar{u}u\rangle, \qquad b = \langle g_c^2 G^2\rangle, \qquad \langle\bar{u}g_c\sigma\cdot Gu\rangle = -m_0^2\langle\bar{u}u\rangle. \tag{33}$$

The quark charge factors e_q are given in units of electric charge

$$e_u = 2/3, \qquad e_d = -1/3, \qquad e_s = -1/3. \tag{34}$$

Note that we choose to keep the quark charge factors explicit in the sum rules. The advantage is that it can facilitate the study of individual quark contribution to the magnetic moments. The parameters f and ϕ account for the flavor-symmetry breaking of the strange quark in the condensates and susceptibilities:

$$f = \frac{\langle\bar{s}s\rangle}{\langle\bar{u}u\rangle} = \frac{\langle\bar{s}g_c\sigma\cdot Gs\rangle}{\langle\bar{u}g_c\sigma\cdot Gu\rangle}, \qquad \phi = \frac{\chi_s}{\chi} = \frac{\kappa_s}{\kappa} = \frac{\xi_s}{\xi}. \tag{35}$$

The anomalous dimension corrections of the interpolating fields and the various operators are taken into account in the leading logarithmic approximation via the factor

$$L^\gamma = \left[\frac{\alpha_s(\mu^2)}{\alpha_s(M^2)}\right]^\gamma = \left[\frac{\ln(M^2/\Lambda_{\rm QCD}^2)}{\ln(\mu^2/\Lambda_{\rm QCD}^2)}\right]^\gamma, \tag{36}$$

where $\mu = 500$ MeV is the renormalization scale and $\Lambda_{\rm QCD}$ is the QCD scale parameter. As usual, the pure excited-state contributions are modeled using terms on the OPE side surviving $M^2 \to \infty$ under the assumption of duality, and are represented by the factors

$$E_n(w) = 1 - e^{-w^2/M^2}\sum_n \frac{(w^2/M^2)^n}{n!}, \tag{37}$$

where w is an effective continuum threshold, and it is in principle different for different sum rules. We will treat it as a free parameter in the analysis.

Now we are ready to present the coefficients defined in Eq. (32). We did eight separate computations, one for each member of the octet. But, we only need to give the coefficients for $\Sigma^+(uus)$, $\Xi^0(ssu)$, and $\Lambda(uds)$. The coefficients for the other members can be obtained from these three by making appropriate substitutions to be specified below.

For Σ^+ at WE_1:

$$\begin{aligned}
c_1 &= \frac{1}{16}[(1+\beta)^2 e_s - 2(3+2\beta+3\beta^2)e_u];\\
c_2 &= \frac{1}{16}(1+\beta)[(-1+3\beta)e_s f_s\phi - 2(1+3\beta)e_u];\\
c_3 &= \frac{1}{12}(-1+\beta)[(1+\beta)e_s f_s\phi - 2e_u(1-\beta+f_s+\beta f_s)];\\
c_4 &= -\frac{1}{384}[(3-2\beta+3\beta^2)e_s + 2(11+6\beta+11\beta^2)e_u];\\
c_5 &= \frac{1}{24}[(3-18\beta+3\beta^2-2f_s+2\beta^2 f_s)e_s + (-5+2\beta+27\beta^2-9f_s+6\beta f_s+27\beta^2 f_s)e_u];\\
c_6 &= -\frac{1}{24}(-1+\beta)[(1+\beta)e_s f_s\phi(8\kappa-\xi) + 2e_u(4\kappa+6\beta\kappa+\xi)];\\
c_7 &= \frac{1}{72}(-1+\beta)[e_s(-3+3\beta+2f_s+2\beta f_s) + 2e_u(-1+\beta+8f_s+8\beta f_s)];\\
c_8 &= -\frac{1}{72}(-1+\beta)[(1+\beta)e_s f_s\phi(8\kappa-\xi) + e_u(-2\kappa+2\beta\kappa+10f_s\kappa+10\beta f_s\kappa+\xi-\beta\xi+f_s\xi+\beta f_s\xi)];\\
c_9 &= -\frac{1}{288}[(7(1+\beta)e_s f_s\phi - e_u(3-3\beta+f_s+\beta f_s)];\\
c_{10} &= -\frac{1}{96}[(1-14\beta+\beta^2)e_s + (-23-2\beta+13\beta^2)e_u(1+f_s)].
\end{aligned} \tag{38}$$

For Ξ^0 at WE_1:

$$
\begin{aligned}
c_1 &= \frac{1}{16}[(1+\beta)^2 e_u - 2(3+2\beta+3\beta^2)e_s];\\
c_2 &= \frac{1}{16}(1+\beta)[(-1+3\beta)e_u - 2(1+3\beta)e_s f_s \phi];\\
c_3 &= \frac{1}{12}(-1+\beta)[(1+\beta)e_u f_s - 2e_s f_s \phi(f_s - \beta f_s + 1 + \beta)];\\
c_4 &= -\frac{1}{384}[(3-2\beta+3\beta^2)e_u + 2(11+6\beta+11\beta^2)e_s];\\
c_5 &= \frac{1}{24}[((3-18\beta+3\beta^2)f_s - 2 + 2\beta^2)e_s + ((-5+2\beta+27\beta^2)f_s - 9 + 6\beta + 27\beta^2)e_s];\\
c_6 &= -\frac{1}{24}(-1+\beta)[(1+\beta)e_u(8\kappa - \xi) + 2e_s f_s \phi(4\kappa + 6\beta\kappa + \xi)];\\
c_7 &= \frac{1}{72}(-1+\beta)[e_u f_s((-3+3\beta)f_s + 2 + 2\beta) + 2e_s f_s((-1+\beta)f_s + 8 + 8\beta)];\\
c_8 &= -\frac{1}{72}(-1+\beta)[(1+\beta)e_u f_s(8\kappa - \xi) + e_s f_s \phi(-2\kappa f_s + 2\beta\kappa f_s + 10\kappa + 10\beta\kappa + \xi - \beta f_s \xi + f_s \xi + \beta\xi)];\\
c_9 &= -\frac{1}{288}[(7(1+\beta)e_u f_s - e_s f_s \phi((3-3\beta)f_s + 1 + \beta)];\\
c_{10} &= -\frac{1}{96}[(1-14\beta+\beta^2)e_u + (-23-2\beta+13\beta^2)e_s(1+f_s)].
\end{aligned}
\tag{39}
$$

For Λ at WE_1:

$$
\begin{aligned}
c_1 &= -\frac{1}{48}((-1+\beta)^2(e_d+e_u) + (13+10\beta+13\beta^2)e_s);\\
c_2 &= \frac{1}{16}(1+\beta)((-1+\beta)(e_d+e_u) - (1+5\beta)e_s f_s \phi);\\
c_3 &= \frac{1}{72}(-1+\beta)((e_d+e_u)(1-\beta+f_s+5\beta f_s) - 2(5+\beta)e_s f_s \phi);\\
c_4 &= -\frac{1}{1152}((17+2\beta+17\beta^2)(e_d+e_u) + (41+26\beta+41\beta^2)e_s);\\
c_5 &= \frac{1}{144}(e_s(-78+\beta(84-16f_s)+\beta^2(210-4f_s)+20f_s) + (-1+\beta)(e_d+e_u)(7+3f_s+\beta(41+33f_s)));\\
c_6 &= -\frac{1}{72}(-1+\beta)(e_s f_s \phi(8(1+2\beta)\kappa + (5+\beta)\xi) + (e_d+e_u)((20+22\beta)\kappa - (1+2\beta)\xi));\\
c_7 &= \frac{1}{216}(-1+\beta)(e_s(39+33\beta-10f_s-2\beta f_s) + (e_d+e_u)(1-\beta+4f_s+20\beta f_s));\\
c_8 &= -\frac{1}{432}(-1+\beta)(2e_s f_s \phi(8(1+2\beta)\kappa + (5+\beta)\xi) + (e_d+e_u)(2(19+17\beta+f_s+5\beta f_s)\kappa\\
&\quad - (1-\beta+f_s+5\beta f_s)\xi));\\
c_9 &= -\frac{1}{576}(-1+\beta)((e_d+e_u)(5+3\beta+3f_s+7\beta f_s) - 2(5+\beta)e_s f_s \phi);\\
c_{10} &= \frac{1}{192}((62-4\beta-34\beta^2)e_s - (-7-10\beta+5\beta^2)(e_d+e_u)(1+f_s)).
\end{aligned}
\tag{40}
$$

At the structure WO_1, the sum rules can be expressed in the following form:

$$
\begin{aligned}
&c_1 m_s L^{-8/9} E_2(w) M^4 + c_2 \chi a L^{-16/27} E_2(w) M^4 + (c_3+c_4) a E_1(w) M^2 + c_5 m_s \chi a^2 L^{-16/27} E_0(w) + c_6 \chi a b L^{-16/27} E_0(w)\\
&\quad + (c_7+c_8) m_s a^2 \frac{1}{M^2} + c_9 a b \frac{1}{M^2} = -\tilde{\lambda}_N^2 m_N \left[\frac{2\mu_N}{M^2} + \frac{\mu_N - 1}{m_N^2} + A\right] e^{-m_N^2/M^2}.
\end{aligned}
\tag{41}
$$

For Σ^+ at WO_1:

$$
\begin{aligned}
c_1 &= -\frac{1}{2}(-1+\beta)((1+\beta)e_s - 2e_u);\\
c_2 &= -\frac{1}{24}(-1+\beta)[(-1+\beta)e_s f_s \phi + 18(1+\beta)e_u];\\
c_3 &= \frac{1}{24}(-1+\beta)[e_s(-6-6\beta-f_s+\beta f_s) - 6e_u(2+2\beta-f_s+\beta f_s)];\\
c_4 &= \frac{1}{96}(-1+\beta)[(-1+\beta)e_s f_s \phi(14\kappa - 13\xi) - 18(1+\beta)e_u(2\kappa+\xi)];\\
c_5 &= -\frac{1}{12}[(3+2\beta+3\beta^2)e_s f_s \phi - (3+4\beta+9\beta^2)e_u(1+f_s)];\\
c_6 &= \frac{1}{576}(-1+\beta)[(-1+\beta)e_s f_s \phi - 18(1+\beta)e_u];\\
c_7 &= -\frac{1}{36}[e_s(-3+3\beta^2+5f_s-2\beta f_s+5\beta^2 f_s) - e_u(3+4\beta+9\beta^2-3f_s+10\beta f_s+9\beta^2 f_s)];\\
c_8 &= -\frac{1}{144}[e_s f_s \phi(4\kappa+8\beta\kappa+4\beta^2\kappa+\xi-10\beta\xi+\beta^2\xi) - e_u(-(3+4\beta+9\beta^2)(1+f_s)\xi\\
&\quad + 4(2\beta+6\beta^2+3f_s+2\beta f_s+3\beta^2 f_s)\kappa)];\\
c_9 &= -\frac{1}{576}[3e_s - e_u(-3+3\beta^2-f_s+2\beta f_s)].
\end{aligned}
\tag{42}
$$

For Ξ^0 at WO_1:

$$
\begin{aligned}
c_1 &= -\frac{1}{2}(-1+\beta)((1+\beta)e_u - 2e_s);\\
c_2 &= -\frac{1}{24}(-1+\beta)[(-1+\beta)e_u + 18(1+\beta)e_s f_s \phi];\\
c_3 &= \frac{1}{24}(-1+\beta)[e_u((-6-6\beta)f_s - 1 + \beta) - 6e_s((2+2\beta)f_s - 1 + \beta)];\\
c_4 &= \frac{1}{96}(-1+\beta)[(-1+\beta)e_u(14\kappa - 13\xi) - 18(1+\beta)e_s f_s \phi(2\kappa+\xi)];\\
c_5 &= -\frac{1}{12}[(3+2\beta+3\beta^2)e_u - (3+4\beta+9\beta^2)e_s f_s \phi(1+f_s)];\\
c_6 &= \frac{1}{576}(-1+\beta)[(-1+\beta)e_u - 18(1+\beta)e_s f_s \phi];\\
c_7 &= -\frac{1}{36}[e_u f_s((-3+3\beta^2)f_s + 5 - 2\beta + 5\beta^2) - e_s f_s((3+4\beta+9\beta^2)f_s - 3 + 10\beta + 9\beta^2)];\\
c_8 &= -\frac{1}{144}[e_u f_s(4\kappa+8\beta\kappa+4\beta^2\kappa+\xi-10\beta\xi+\beta^2\xi) - e_s f_s \phi(-(3+4\beta+9\beta^2)(1+f_s)\xi\\
&\quad + 4((2\beta+6\beta^2)f_s + 3 + 2\beta + 3\beta^2)\kappa)];\\
c_9 &= -\frac{1}{576}[3e_u - e_s((-3+3\beta^2)f_s - 1 + 2\beta)].
\end{aligned}
\tag{43}
$$

For Λ at WO_1:

$$
\begin{aligned}
c_1 &= -\frac{1}{6}(-1+\beta)((e_d+e_u)(1+2\beta)-(5+\beta)e_s);\\
c_2 &= -\frac{1}{72}(-1+\beta)((7+11\beta)(e_d+e_u)+(37+35\beta)e_s f_s\phi);\\
c_3 &= -\frac{1}{72}(-1+\beta)((e_d+e_u)(14+\beta(22-3f_s)+3f_s)+e_s(-30-6\beta+35f_s+37\beta f_s));\\
c_4 &= \frac{1}{288}(-1+\beta)((e_d+e_u)(2(-23+5\beta)\kappa+(17-35\beta)\xi)-e_s f_s\phi(58\kappa+86\beta\kappa+49\xi+23\beta\xi));\\
c_5 &= \frac{1}{24}((-1+\beta^2)(e_d+e_u)(1+f_s)+2(5+6\beta+13\beta^2)e_s f_s\phi);\\
c_6 &= -\frac{1}{1728}((-1+\beta)((11+7\beta)(e_d+e_u)+(35+37\beta)e_s f_s\phi));\\
c_7 &= \frac{1}{216}(-(-1+\beta)(e_d+e_u)(-7+\beta-f_s+13\beta f_s)+e_s(-30+34f_s+4\beta(6+7f_s)+\beta^2(6+82f_s)));\\
c_8 &= \frac{1}{864}(2e_s f_s\phi(4(7+10\beta+19\beta^2)\kappa-(11+26\beta+35\beta^2)\xi)+(-1+\beta)(e_d+e_u)(4(-4-2\beta+5f_s+7\beta f_s)\kappa\\
&\quad -(-5+11\beta)(1+f_s)\xi));\\
c_9 &= \frac{1}{3456}((-1+\beta)(2(5+\beta)e_s+(e_d+e_u)(5+\beta+11f_s+13\beta f_s))).
\end{aligned}
\tag{44}
$$

At the structure WO_2, the sum rules can be expressed in the following form:

$$
\begin{aligned}
&c_1 m_s L^{-8/9}E_1(w)M^2+c_2\chi a L^{-16/27}E_1(w)M^2+(c_3+c_4)aE_0(w)+c_5 m_s\chi a^2 L^{-16/27}E_0(w)+c_6 m_0^2 a L^{-4/9}\frac{1}{M^2}\\
&\quad +c_7\chi ab L^{-16/27}\frac{1}{M^2}+(c_8+c_9)m_s a^2\frac{1}{M^4}+c_{10}ab\frac{1}{M^4}=-\frac{\tilde{\lambda}_N^2}{m_N}\left[\frac{2(\mu_N-1)}{M^2}+A\right]e^{-m_N^2/M^2}.
\end{aligned}
\tag{45}
$$

For Σ^+ at WO_2:

$$
\begin{aligned}
c_1 &= -\frac{1}{2}(-1+\beta)[(1+\beta)e_s-2e_u];\\
c_2 &= -\frac{1}{6}(-1+\beta)^2 e_s f_s\phi;\\
c_3 &= -\frac{1}{4}(-1+\beta)[e_s(2+2\beta-f_s+\beta f_s)+2e_u(-2-2\beta-f_s+\beta f_s)];\\
c_4 &= \frac{1}{16}(-1+\beta)[e_s f_s\phi+2(1+\beta)e_u](2\kappa-\xi);\\
c_5 &= -\frac{1}{3}(-1+\beta)[2e_s f_s\phi+e_u(-1-\beta-f_s+\beta f_s)];\\
c_6 &= \frac{1}{24}(-1+\beta)[7(1+\beta)e_s+e_u(-1-\beta-3f_s+3\beta f_s)];\\
c_7 &= -\frac{1}{144}(-1+\beta)^2 e_s f_s\phi;\\
c_8 &= \frac{1}{18}[e_s(-3+3\beta^2+5f_s-2\beta f_s+5\beta^2 f_s)-e_u(3+4\beta+9\beta^2-3f_s+10\beta f_s+9\beta^2 f_s)];\\
c_9 &= \frac{1}{72}[e_s f_s\phi((1-10\beta+\beta^2)\xi+4(1+\beta)^2\kappa)-e_u(4(2\beta+6\beta^2+3f_s+2\beta f_s+3\beta^2 f_s)\kappa\\
&\quad -(3+4\beta+9\beta^2)(1+f_s)\xi)];\\
c_{10} &= -\frac{1}{288}(-1+\beta)((1+\beta)e_s-e_u(-3-3\beta-f_s+\beta f_s)].
\end{aligned}
\tag{46}
$$

For Ξ^0 at WO_2:

$$
\begin{aligned}
c_1 &= -\frac{1}{2}(-1+\beta)[(1+\beta)e_u - 2e_s];\\
c_2 &= -\frac{1}{6}(-1+\beta)^2 e_u;\\
c_3 &= -\frac{1}{4}(-1+\beta)[e_u f_s((2+2\beta)f_s - 1 + \beta) + 2e_s f_s(-(2+2\beta)f_s - 1 + \beta)];\\
c_4 &= \frac{1}{16}(-1+\beta)[e_s f_s \phi + 2(1+\beta)e_u](2\kappa - \xi);\\
c_5 &= -\frac{1}{3}(-1+\beta)[2e_u f_s + e_s f_s \phi(-(1+\beta)f_s - 1 + \beta)];\\
c_6 &= \frac{1}{24}(-1+\beta)[7(1+\beta)e_u f_s + e_s(-(1+\beta)f_s - 3 + 3\beta)];\\
c_7 &= -\frac{1}{144}(-1+\beta)^2 e_u;\\
c_8 &= \frac{1}{18}[e_u f_s((-3+3\beta^2)f_s + 5 - 2\beta + 5\beta^2) - e_s f_s((3+4\beta+9\beta^2)f_s - 3 + 10\beta + 9\beta^2)];\\
c_9 &= \frac{1}{72}[e_u f_s((1-10\beta+\beta^2)\xi + 4(1+\beta)^2\kappa) - e_s f_s(4((2\beta+6\beta^2)f_s + 3 + 2\beta + 3\beta^2)\kappa\\
&\quad - (3+4\beta+9\beta^2)(1+f_s)\xi)];\\
c_{10} &= -\frac{1}{288}(-1+\beta)((1+\beta)e_u - e_s(-(3+3\beta)f_s - 1 + \beta)].
\end{aligned}
\tag{47}
$$

For Λ at WO_2:

$$
\begin{aligned}
c_1 &= -\frac{1}{12}(-1+\beta)((e_d+e_u)(1+2\beta) - (5+\beta)e_s);\\
c_2 &= -\frac{1}{36}(-1+\beta)^2(2(e_d+e_u) - e_s f_s \phi);\\
c_3 &= \frac{1}{24}(-1+\beta)((e_d+e_u)(2+\beta(-6+f_s) - f_s) + +e_s(10 + 3f_s + \beta(2+5f_s)));\\
c_4 &= \frac{1}{96}(-1+\beta)((-1+3\beta)(e_d+e_u) + (5+3\beta)e_s f_s \phi)(2\kappa - \xi);\\
c_5 &= \frac{1}{12}(-1+\beta)((e_d+e_u)(-1+\beta(-1+f_s) - f_s) + 4e_s f_s \phi);\\
c_6 &= \frac{1}{96}(-1+\beta)(-2(5+\beta)e_s + (e_d+e_u)(3+7\beta+5f_s+3\beta f_s));\\
c_7 &= -\frac{1}{864}(-1+\beta)^2(2(e_d+e_u) - e_s f_s \phi);\\
c_8 &= \frac{1}{216}((-1+\beta)(e_d+e_u)(-7+\beta - f_s + 13\beta f_s) - 2e_s(-15 + 17f_s + 2\beta(6+7f_s) + \beta^2(3+41f_s)));\\
c_9 &= \frac{1}{864}(2e_s f_s \phi(-4(7+10\beta+19\beta^2)\kappa + (11+26\beta+35\beta^2)\xi) - (-1+\beta)(e_d+e_u)(4(-4-2\beta+5f_s+7\beta f_s)\kappa\\
&\quad - (-5+11\beta)(1+f_s)\xi));\\
c_{10} &= -\frac{1}{3456}((-1+\beta)(2(5+\beta)e_s + (e_d+e_u)(5+\beta+11f_s+13\beta f_s)).
\end{aligned}
\tag{48}
$$

The coefficients for the other five members of the octet family can be obtained from them in the following way:

(i) For proton p, replace the s quark by the d quark in Σ^+.

(ii) For neutron n, exchange the d quark with the u quark in proton p.

(iii) For Σ^-, replace the u quark by the d quark in Σ^+.

(iv) For Ξ^-, replace the u quark by the d quark in Ξ^0.

(v) For Σ^0, they can be obtained through the relation [19] $c(\Sigma^0) = \frac{2}{3}c(\Lambda_{d\leftrightarrow s}) + \frac{2}{3}c(\Lambda_{u\leftrightarrow s}) - \frac{1}{3}c(\Lambda)$ in each coefficient.

Here the conversions between u and d quarks are achieved by simply switching their charge factors e_u and e_d. The conversions from s quark to u or d quarks involve setting $m_s = 0, f = \phi = 1$, in addition to the switching of charge factors. These relations are inherent in the master formulas Eqs. (24) and (25). We have used our eight separate calculations to check that these rules indeed work. They also provide nontrivial checks of our algebra.

At this point, we can make some comparisons with previous calculations in Refs. [5–7]. First, we use general interpolating fields where we can vary β to achieve the best match in the sum rules. The previous calculations correspond to a fixed value of $\beta = -1$. This effect was studied in detail in Ref. [20], and it was found that $\beta = -1.2$ is the optimal value. Most of our results are at $\beta = -1.2$. Second, we have checked that our sum rules agree with those in the previous calculations for the most part. For example, for the proton at WE_1, we completely agree except for the $\kappa - 2\xi$ term in Eq. (2.16) in Ref. [5]. In all of our sum rules, we have the combination $2\kappa - \xi$ instead of $\kappa - 2\xi$. For the strange members (Σ, Ξ, Λ), they have eight terms in the OPE, while we have 10 terms. For the sum rules at structure WO_1, they have only three terms, while we have nine terms. For the sum rules at structure WO_2, they have only four terms, while we have 10 terms. Third, they only analyzed the sum rules at structure WE_1, while we will examine all the structures. Fourth, we use a completely different analysis method.

Before going into the analysis, we would like to point out some relations among the correlation functions (or OPE) based on symmetries, which lead to the same relations in the magnetic moments. In exact SU(3)-flavor symmetry, it is known that the magnetic moments of the octet family are related by (see, for example, Ref. [21])

$$\mu_{\Sigma^+} = \mu_p, \qquad 2\mu_\Lambda = \mu_n, \qquad \mu_{\Sigma^-} + \mu_n = -\mu_p, \qquad \mu_{\Xi^-} = \mu_{\Sigma^-}, \qquad \mu_{\Xi^0} = \mu_n. \tag{49}$$

These relations are borne out in the OPE of our sum rules if SU(3)-flavor symmetry is enforced. They are only approximately true since SU(3)-flavor symmetry is broken by the strange quark. Here we have the advantage of studying the symmetry-breaking effects since the terms are explicit in our QCD sum rules.

IV. SUM RULE ANALYSIS

The sum rules for magnetic moments have the generic form of OPE-ESC = pole + transition, or

$$\Pi_{\rm mag}(\text{QCD}, \beta, w, M^2) = \tilde{\lambda}_N^2\left(\frac{\mu_N}{M^2} + A\right)e^{-m_N^2/M^2}, \tag{50}$$

where QCD represents all the QCD input parameters. The task then becomes, given the function $\Pi_{\rm mag}$ with known QCD input parameters and the ability to vary β, find the phenomenological parameters (magnetic moment μ_N, transition strength A, coupling strength $\tilde{\lambda}_N^2$, and continuum threshold w) by matching the two sides over some region in the Borel mass M. A χ^2 minimization is best suited for this purpose. It turns out that there are too many fit parameters for this procedure to be successful in general. To alleviate the situation, we employ the corresponding mass sum rules which have a similar generic form of OPE-ESC = pole, or

$$\Pi_{\rm mass}(\text{QCD}, \beta, w_1, M^2) = \tilde{\lambda}_N^2 e^{-m_N^2/M^2}, \tag{51}$$

which shares some of the common parameters. Note that the continuum threshold may not be the same in the two sum rules. By taking the ratio of the two equations, we are left with

$$\frac{\Pi_{\rm mag}(\text{QCD}, \beta, w, M^2)}{\Pi_{\rm mass}(\text{QCD}, \beta, w_1, M^2)} = \frac{\mu_N}{M^2} + A. \tag{52}$$

This is the form we are going to implement. By plotting the two sides as a function of $1/M^2$, the slope will be the magnetic moment and the intercept the transition strength. The linearity (or deviation from it) of the left-hand side gives an indication of OPE convergence and the role of excited states. The two sides are expected to match for a good sum rule. This way of matching the sum rules has two advantages. First, the slope, which is the magnetic moment of interest, is usually better determined than the intercept. Second, by allowing the possibility of different continuum thresholds, we ensure that both sum rules stay in their valid regimes.

We use the chiral-even mass sum rules in Ref. [22] which are listed here in the same notation,

$$\begin{aligned} &p_1 L^{-4/9} E_3(w_1) M^6 + p_2 b L^{-4/9} E_1(w_1) M^2 + p_3 m_s a L^{4/9} \\ &\quad + p_4 a^2 L^{4/9} + p_5 a^2 k_v L^{4/9} + p_6 m_0^2 a^2 L^{-2/27}\frac{1}{M^2} \\ &= \tilde{\lambda}_N^2 e^{-m_N^2/M^2}. \end{aligned} \tag{53}$$

The coefficients for N are

$$\begin{aligned} &p_1 = \frac{1}{64}(5 + \beta + 5\beta^2); \qquad p_2 = \frac{1}{256}(5 + \beta + 5\beta^2); \\ &p_3 = 0; \qquad p_4 = \frac{1}{24}(7 - 2\beta - 5\beta); \qquad p_5 = 0; \\ &p_6 = -\frac{1}{96}(13 - 2\beta - 11\beta^2). \end{aligned} \tag{54}$$

For Λ:

$$
\begin{aligned}
p_1 &= \frac{1}{64}(5 + 2\beta + 5\beta^2);\\
p_2 &= \frac{1}{256}(5 + 2\beta + 5\beta^2);\\
p_3 &= \frac{1}{96}((20 - 15f_s) - (16 + 6f_s)\beta - (4 + 15f_s)\beta^2);\\
p_4 &= \frac{1}{96}((4f_s - 5 - 6t) + (4 + 4f_s)\beta + (4f_s + 1 \\
&\quad + 6t)\beta^2);\\
p_5 &= \frac{1}{72}((10f_s + 11) + (2 - 8f_s)\beta - (2f_s + 13)\beta^2);\\
p_6 &= \frac{1}{288}((-16f_s - 23) + (8f_s - 2)\beta + (8f_s + 25)\beta^2).
\end{aligned} \tag{55}
$$

For Σ:

$$
\begin{aligned}
p_1 &= \frac{1}{64}(5 + 2\beta + 5\beta^2);\\
p_2 &= \frac{1}{256}(5 + 2\beta + 5\beta^2);\\
p_3 &= \frac{1}{32}((12 - 5f_s) - 2f_s\beta - (12 + 5f_s)\beta^2);\\
p_4 &= -\frac{1}{94}((4f_s + 21 + 18t) + 4f_s\beta + (4f_s - 21 \\
&\quad - 18t)\beta^2);\\
p_5 &= \frac{1}{24}((6f_s + 1) - 2\beta - (6f_s - 1)\beta^2);\\
p_6 &= -\frac{1}{96}((12f_s + 1) - 2\beta - (12f_s - 1)\beta^2).
\end{aligned} \tag{56}
$$

For Ξ:

$$
\begin{aligned}
p_1 &= \frac{1}{64}(5 + 2\beta + 5\beta^2);\\
p_2 &= \frac{1}{256}(5 + 2\beta + 5\beta^2);\\
p_3 &= \frac{3}{16}((2 - f_s) - 2f_s\beta - (2 + f_s)\beta^2);\\
p_4 &= -\frac{1}{96}((15 - f_s + 18t) - 10f_s\beta - (15 + f_s \\
&\quad + 18t)\beta^2);\\
p_5 &= \frac{1}{24}f_s((f_s + 6) - 2f_s\beta + (f_s - 6)\beta^2);\\
p_6 &= -\frac{1}{94}f_s((f_s + 12) - 2f_s\beta + (f_s - 12)\beta^2).
\end{aligned} \tag{57}
$$

The function t is defined as $t \equiv \ln\frac{M^2}{\mu^2} - \gamma_{\rm EM}$ with $\gamma_{\rm EM} \approx 0.577$ as the Euler-Mascheroni constant.

We use the Monte Carlo procedure first introduced in Ref. [20] to carry out the search which allows a rigorous error analysis. In this method, the entire phase space of the input QCD parameters is explored simultaneously and is mapped into uncertainties in the phenomenological parameters. This leads to more realistic uncertainty estimates than traditional approaches.

First, a set of randomly selected, Gaussianly distributed condensates are generated with assigned uncertainties. Here we give 10% for the uncertainties of input parameters, and this number can be adjusted to test the sensitivity of the QCD parameters. Then the OPE is constructed in the Borel window with evenly distributed points M_j. Note that the uncertainties in the OPE are not uniform throughout the Borel window. They are larger at the lower end where uncertainties in the higher-dimensional condensates dominate. Thus, it is crucial that the appropriate weight is used in the calculation of χ^2. For the OPE obtained from the kth set of QCD parameters, the χ^2 per degree of freedom is

$$
\frac{\chi_k^2}{N_{\rm DF}} = \sum_{j=1}^{n_B} \frac{[\Pi_k^{\rm OPE}(M_j^2, \beta, w, w_1) - \Pi_k^{\rm Phen}(M_j^2, \mu, A)]^2}{(n_B - n_p)\sigma_{\rm OPE}^2(M_j)}, \tag{58}
$$

where $\Pi^{\rm OPE}$ refers to the LHS of Eq. (52) and $\Pi^{\rm Phen}$ its RHS. The integer n_p is the number of phenomenological search parameters. In this work, $n_B = 51$ points were used along the Borel axis. The procedure is repeated for many QCD parameter sets, resulting in distributions for phenomenological fit parameters, from which errors are derived. In practice, 200 configurations are sufficient for getting stable uncertainties. We used about 2000 sets to resolve more subtle correlations among the QCD parameters and the phenomenological fit parameters. This means that each sum rule is fitted 2000 times to arrive at the final results.

The QCD input parameters are given as follows. The condensates are taken as $a = 0.52\ {\rm GeV}^3$, $b = 1.2\ {\rm GeV}^4$, and $m_0^2 = 0.72\ {\rm GeV}^2$. For the factorization violation parameter, we use $\kappa_v = 2.0$. The QCD scale parameter is restricted to $\Lambda_{\rm QCD} = 0.15$ GeV. The vacuum susceptibilities have been estimated in studies of nucleon magnetic moments [3,5,9,12], but the values vary depending on the method used. We use $\chi = -6.0\ {\rm GeV}^{-2}$ and $\kappa = 0.75$, $\xi = -1.5$. Note that χ is almost an order of magnitude larger than κ and ξ and is the most important of the three. The strange quark parameters are placed at $m_s = 0.15$ GeV, $f = 0.83$, and $\phi = 0.60$ [6,9]. These input parameters are just central values. We will explore sensitivity to these parameters by assigning uncertainties to them in the Monte Carlo analysis.

V. RESULTS AND DISCUSSION

We have 24 sum rules in total to analyze: three for each member of the octet. For each sum rule, we have in principle five parameters to determine: μ, A, w, w_1, and β. But a search treating all five parameters as free does not work because there is not enough information in the OPE.

In fact, the freedom to vary β can be used as an advantage to yield the optimal match. We find that $\beta = -1.2$ gives the best match in most cases. This agrees with the value suggested in Ref. [20]. One exception is the proton: we found a better solution at $\beta = -0.4$ than at $\beta = -1.2$. Another parameter that can be used to our advantage is the continuum threshold w_1 for the corresponding mass sum rule. We fix it to the value that gives the best solution to the mass sum rule independently. The following values for w_1 are used: for the nucleon, $w_1 = 1.44$ GeV; for Λ, $w_1 = 1.60$ GeV; for Σ, $w_1 = 1.66$ GeV; for Ξ, $w_1 = 1.82$ GeV. In this way the magnetic moment sum rule and the mass sum rule can stay in their respective valid Borel regimes. This leaves us with three parameters: μ, A, and w. Unfortunately, a three-parameter search is either unstable or returns values for w smaller than the particle mass, an unphysical situation. Again we think this is a symptom of insufficient information in the OPE. So we are forced to fix the continuum threshold w that corresponds to the best match for the central values of the QCD parameters.

A. The sum rule at WE_1

The results determined this way at the WE_1 structure are displayed in Table I. The Borel window is determined by the following two criteria: OPE convergence which gives the lower bound, and ground-state dominance which gives the upper bound. It is done iteratively. For each value of β, we adjust the Borel window until the best solution is found. We see that our calculated magnetic moments agree with experiment fairly well within error bars.

We stress that the errors are derived from Monte Carlo distributions which give the most realistic estimation of the uncertainties. An example of such distributions is given in Fig. 4. We see that they are roughly Gaussian distributions. The central value is taken as the average, and the error is 1 standard deviation of the distribution. We found about 10% accuracy for the magnetic moments in our Monte Carlo analysis, resulting from 10% uniform uncertainty in all the QCD input parameters. Of course, the uncertainties in the QCD parameters can be nonuniform. For example, we tried the uncertainty assignments (which are quite conservative) in Ref. [20], and found about 30% uncertainties in our output.

To gain a better appreciation on how the QCD sum rules produce the results, we show Fig. 5, using the proton as an example. There are three graphs in this figure to give three different aspects of the analysis. The first graph shows how the two sides of Eq. (52) match over the Borel window, which should be linear as a function of $1/M^2$ according to the right-hand side of this equation. Indeed, we observe excellent linear behavior from the OPE side (LHS). The match is almost perfect (barely distinguishable between the solid and dotted lines). The slope gives the magnetic moment μ, and the intercept gives the transition contribution A. We find that the inclusion of A is important in producing the best match. Also plotted are the individual contributions from u and d quarks. We see that for the proton, the u-quark contribution is the dominant one, which is expected because it is doubled represented in the proton (uud). We define the slope from an individual quark contribution as the effective magnetic moment of that quark in the particle.

The second graph in Fig. 5 shows how the various terms in the OPE contribute to the determination of magnetic moments. The M^0 term, which contains the contributions from the condensates χa^2 and b, plays an important role. It is the leading contribution in the region below $M^2 < 1.2$ GeV^2. For this reason, the sum rule at WE_1 is expected to have good spectral properties. Indeed this is confirmed in the third graph where we plot the three terms in the phenomenological side (pole, transition, and excited) as a

TABLE I. Results for the magnetic moment of octet baryons from the QCD sum rule in Eq. (32) (structure WE_1). The seven columns correspond to, from left to right: particle, β value, Borel region in which the two sides of the QCD sum rule are matched, continuum threshold, transition strength, extracted magnetic moment in unit of nuclear magnetons, and experimental value. The errors are derived from 2000 samples in the Monte Carlo analysis with 10% uncertainty on all QCD input parameters.

	β	Region (GeV)	w (GeV)	A (GeV^{-2})	μ_B (μ_N)	Exp. (μ_N)
p	-1.2	0.7–0.9	1.40	1.46 ± 0.34	3.01 ± 0.24	2.79
	-0.4	0.8–1.2	1.60	0.74 ± 0.13	2.82 ± 0.26	2.79
n	-1.2	0.7–1.1	1.40	-0.19 ± 0.09	-1.97 ± 0.15	-1.91
Λ	-1.2	1.1–1.2	1.60	-0.45 ± 0.05	-0.56 ± 0.15	-0.61
Σ^+	-1.2	1.1–1.3	1.85	0.56 ± 0.06	2.31 ± 0.25	2.45
Σ^0	-1.2	1.0–1.6	1.80	0.07 ± 0.02	0.69 ± 0.07	0.65
Σ^-	-1.2	1.3–1.8	1.80	-0.08 ± 0.01	-1.16 ± 0.10	-1.16
Ξ^0	-1.2	1.6–1.9	2.15	-0.16 ± 0.01	-1.15 ± 0.05	-1.25
Ξ^-	-1.2	1.1–1.4	2.00	-0.34 ± 0.02	-0.64 ± 0.06	-0.65

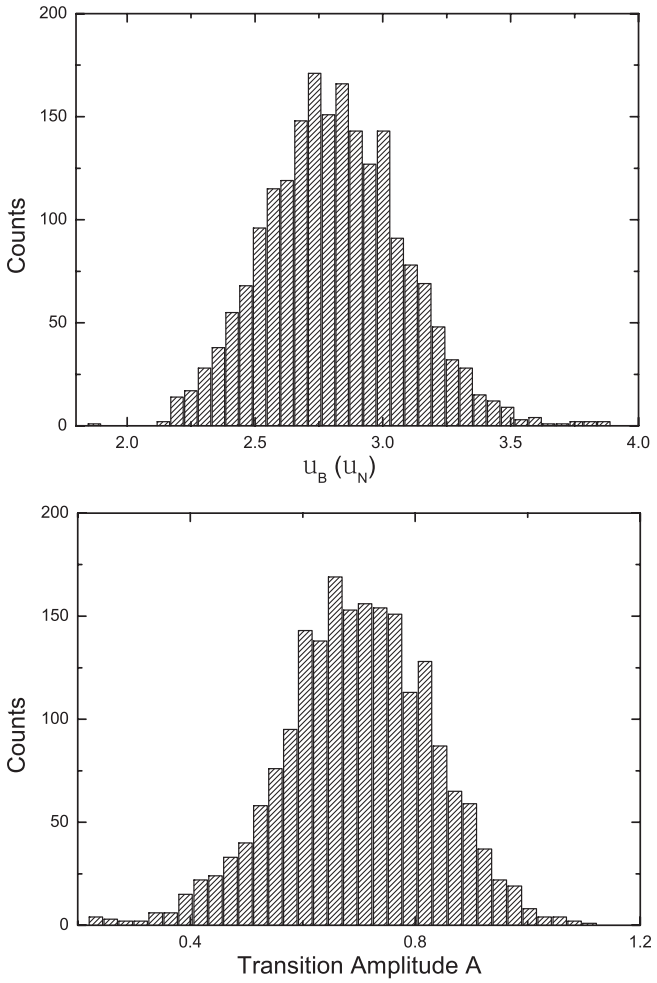

FIG. 4. Histogram for the proton magnetic moment (top panel) and transition amplitude (bottom panel) obtained from Monte Carlo fits of Eq. (32) at WE_1 for 2000 QCD parameter sets. They are based on 10% uncertainty given to all the QCD input parameters.

function of M^2. The ground-state pole is dominant (over 70% of the RHS at the low end of the Borel window). The excited-state contribution starts small, then grows with M^2, as expected from the continuum model. The transition contribution is small in this sum rule. It is consistently smaller than the excited-state contribution and has a weak dependence on the Borel mass.

B. The sum rule at WO_1

Next, we analyze the sum rule in Eq. (41) at the structure WO_1, using the same procedure. Table II displays the results extracted from this sum rule. The magnetic moments have larger errors than those from WE_1: about 15% as opposed to 10%. The agreement with experiment is reasonable (with the exception of Σ^-), but not as good as those from WE_1. We had to search a wider region in β to find the best match. The transition contribution (A) is larger for the strange particles, as well as their errors.

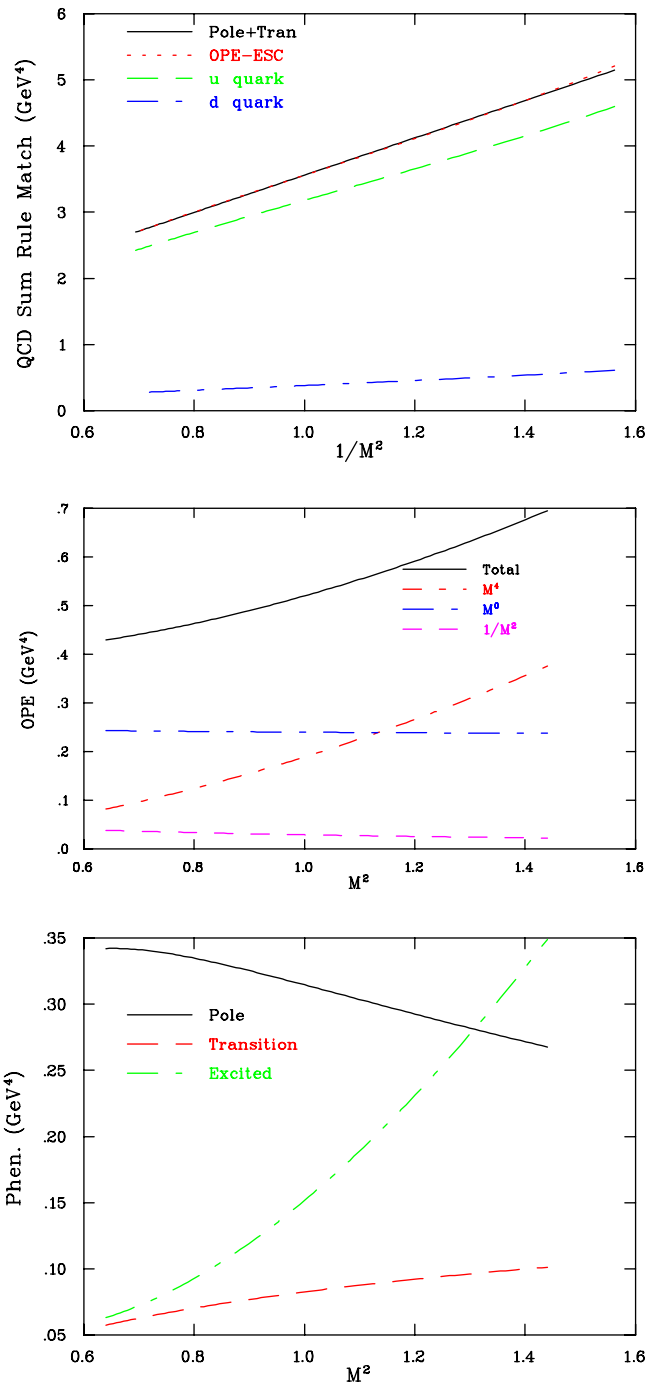

FIG. 5 (color online). Analysis of the QCD sum rule in Eq. (32) (structure WE_1) for the proton at $\beta = -0.4$ according to Eq. (52). In the top panel, the pole plus transition terms (solid lines) are compared against the OPE minus the excited-state contributions (dashed lines) as a function of $1/M^2$ (the two should match for an ideal sum rule). Also plotted are the individual contributions from u (long-dashed lines) and d (dot-dashed lines) quarks. In the middle panel, the total in the OPE side and its various terms are plotted as a function of M^2. In the bottom panel, the three terms in the phenomenological side: pole (solid line), transition (long-dashed line), and excited (dot-dashed line) are plotted as a function of M^2.

TABLE II. Similar to Table I, but for the QCD sum rule in Eq. (41) (structure WO_1).

	β	Region (GeV)	w (GeV)	A (GeV^{-1})	μ_B (μ_N)	Exp. (μ_N)
p	-0.8	1.4–1.6	1.50	1.03 ± 0.16	2.67 ± 0.16	2.79
n	-1.2	1.2–1.4	1.40	-0.54 ± 0.11	-1.70 ± 0.11	-1.91
Λ	-1.2	1.0–1.3	1.60	-2.3 ± 0.31	-0.62 ± 0.17	-0.61
Σ^+	-0.6	1.5–1.7	1.60	1.60 ± 0.50	2.46 ± 0.40	2.45
Σ^0	-1.0	1.4–1.6	1.70	0.23 ± 0.11	0.58 ± 0.09	0.65
Σ^-	-0.6	1.2–1.5	1.60	-2.04 ± 0.34	-0.57 ± 0.26	-1.16
Ξ^0	-1.2	1.2–1.4	2.10	-1.52 ± 0.21	-1.27 ± 0.15	-1.25
Ξ^-	-0.2	1.7–1.8	1.90	-0.4 ± 0.41	-0.49 ± 0.29	-0.65

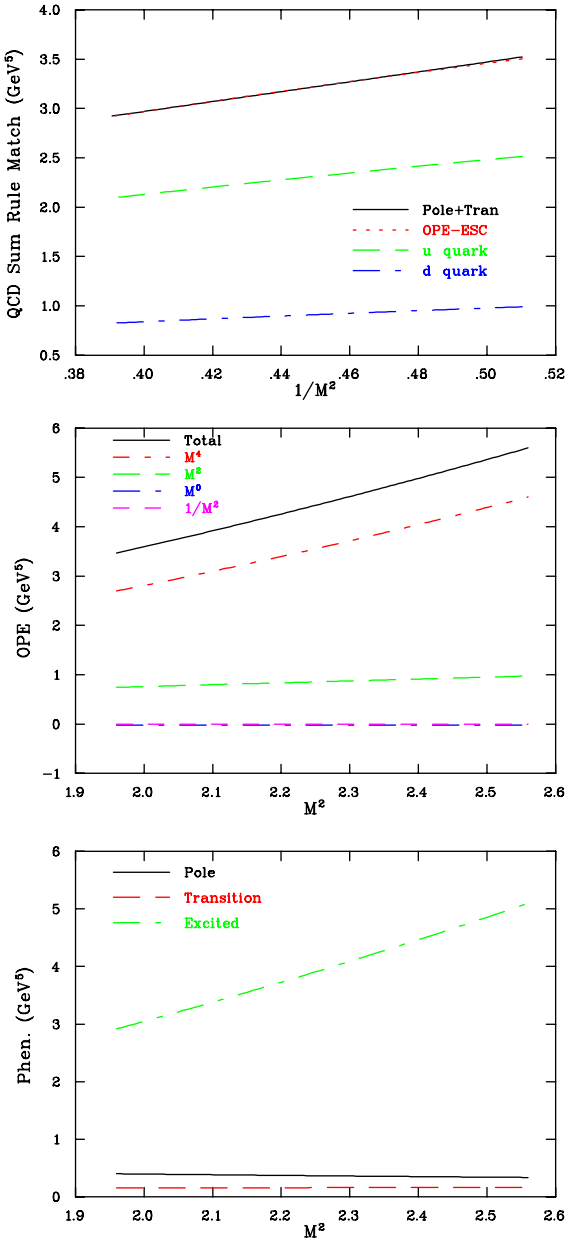

FIG. 6 (color online). Similar to Fig. 5, but at structure WO_1 and $\beta = -1.2$.

Figure 6 shows the details of the analysis in the case of the proton. The matching is very good, as indicated in the top graph. The middle graphs shows that the leading contribution in the OPE (M^4 term) is χa, followed by the quark condensate a (M^2 term). The condensate χab (M^0 term) and ab (M^{-2} term) are very small in this sum rule. The bottom graph reveals a surprising result: the excited-state dominates over the pole and the transition. As a result, this sum rule is less reliable. This is the reason why the results from this sum rule are not as good as those from WE_1. This sum rule also shows the importance of checking the individual terms in the phenomenological side, in addition to looking at the best match of the two sides. In this case, there is no pole dominance, even though the leading term is nonperturbative and the match is almost perfect.

C. The sum rule at WO_2

Finally, we present the results from the sum rule in Eq. (45) at the structure WO_2 in Table III. The agreement with experiment is not as good as the other two sum rules. For example, Σ^- and Ξ^- have the wrong sign. Figure 7 shows the details of the analysis for the proton. The matching is very good, as indicated in the top graph. The middle graph shows that the leading contribution in the OPE is M^2 with a coefficient of χa, followed by the M^0 term. The $1/M^2$ term is slightly negative, while the $1/M^4$ term is very small. The bottom graph shows that the excited state dominates over the pole and the transition, like the sum rule from WO_1, but the relative size of the pole is much larger. Since the WO_2 sum rule has power corrections up to $1/M^4$, it is expected to be more reliable than the WO_1 sum rule. But our analysis shows that this advantage is offset by the smallness of the $1/M^2$ and $1/M^4$ terms. As a result, the reliability of the WO_2 sum rule is about the same as the WO_1 sum rule.

We have performed the same analysis for all the members and all three structures. Figure 8 shows the graphs for the neutron. In this case, the slope is negative. Again, the sum rule at WE_1 has excellent convergence properties. The WO_1 sum rule has a good match, but the pole is less than

TABLE III. Similar to Table I, but for the QCD sum rule in Eq. (45) (structure WO_2).

	β	Region (GeV)	w (GeV)	A (GeV^{-2})	μ_B (μ_N)	Exp. (μ_N)
p	-1.2	1.3–1.4	1.60	0.42 ± 0.07	2.53 ± 0.13	2.79
n	-1.2	1.7–1.9	1.60	0.26 ± 0.03	-1.73 ± 0.28	-1.91
Λ	-1.2	1.3–1.4	1.90	-0.85 ± 0.22	-0.53 ± 0.17	-0.61
Σ^+	-1.0	1.2–1.4	1.70	0.21 ± 0.05	1.50 ± 0.11	2.45
Σ^0	-1.2	1.0–1.6	1.60	-0.02 ± 0.02	1.04 ± 0.07	0.65
Σ^-	-1.2	1.4–1.6	1.65	0.0 ± 0.01	0.61 ± 0.06	-1.16
Ξ^0	-1.2	1.6–2.0	2.1	-0.08 ± 0.03	-1.20 ± 0.23	-1.25
Ξ^-	-1.2	1.4–1.5	2.2	0.22 ± 0.09	0.80 ± 0.21	-0.65

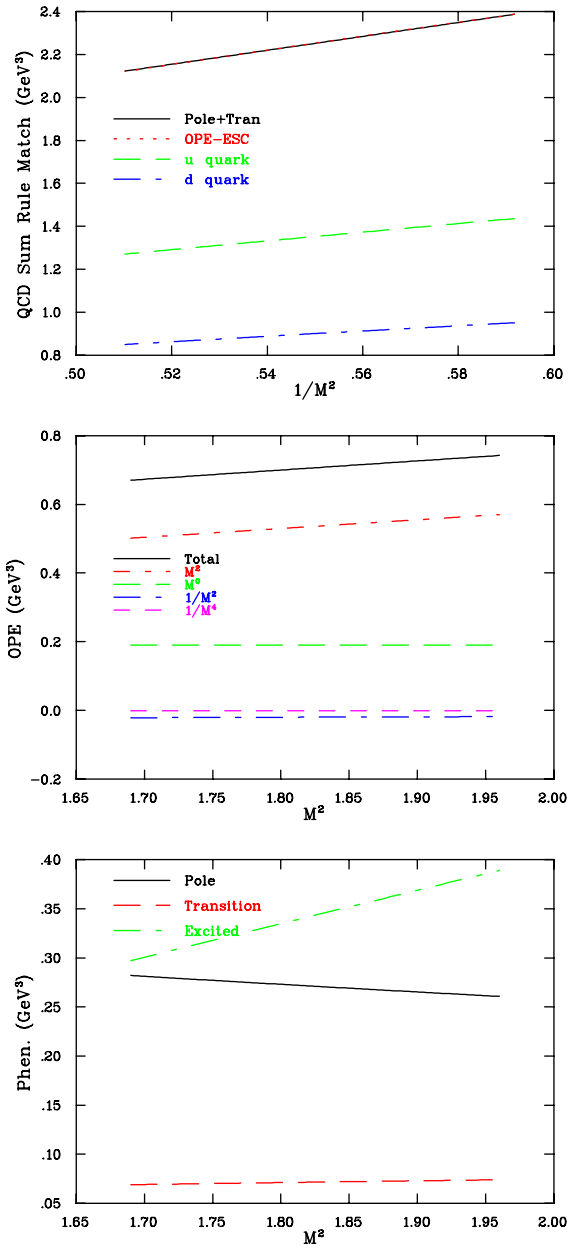

FIG. 7 (color online). Similar to Fig. 5, but at structure WO_2 and $\beta = -1.2$.

the excited state. The WO_2 sum rule does not have a good match. Figure 9 shows the case for the Σ^0, which has all three quark contributions (u, d, and s).

Overall, based on the quality of the match, the broadness of the Borel window and its reach into the lower end in the Borel mass, the size of the continuum contribution, and the OPE convergence, we find that the sum rule at WE_1 is the most reliable of the three sum rules.

D. Some physics discussions

Based on the results of our comprehensive analysis, we conclude that the QCD sum rules at WE_1 in Eq. (5) are the most reliable. Here we discuss some physics implications of the results extracted from them (Table I). First we look at some ratios of magnetic moments listed in Table IV. Here we compare our results with those from the SU(6) symmetry, lattice calculations [23], and experiment. From the table, we see that the QCD sum rule results compare well against other approaches and experiment. They agree a little better with experiment than the lattice results. Furthermore, our QCD rum rule results are an improvement over the ratios from previous QCD sum rule calculations in Ref. [5].

Next, we consider a few sum rules among magnetic moments that have been discussed in the literature. They reveal interesting quark dynamics in the baryons. They are mostly based on SU(6)-symmetry considerations in the quark model. We begin with the sum rule [24]

$$\frac{3(p - \Sigma^+)}{\Xi^- - \Xi^0} = \frac{(p + 3\Lambda)}{p}. \tag{59}$$

It assumed "baryon independence" of quark moments: the independence of which baryon the same quark is in, a concept first mentioned by Franklin [25]. In other words, each quark is not sensitive to the environment it resides in and quarks in different spin states had the same effective moments. In this sum rule, it also assumed that the s quark moment in the Λ is the same as in the Σ and Ξ, even though the spin states are different. This rum rule is violated the most (by a factor of 5) using present values of magnetic moments. This large violation is mostly due to

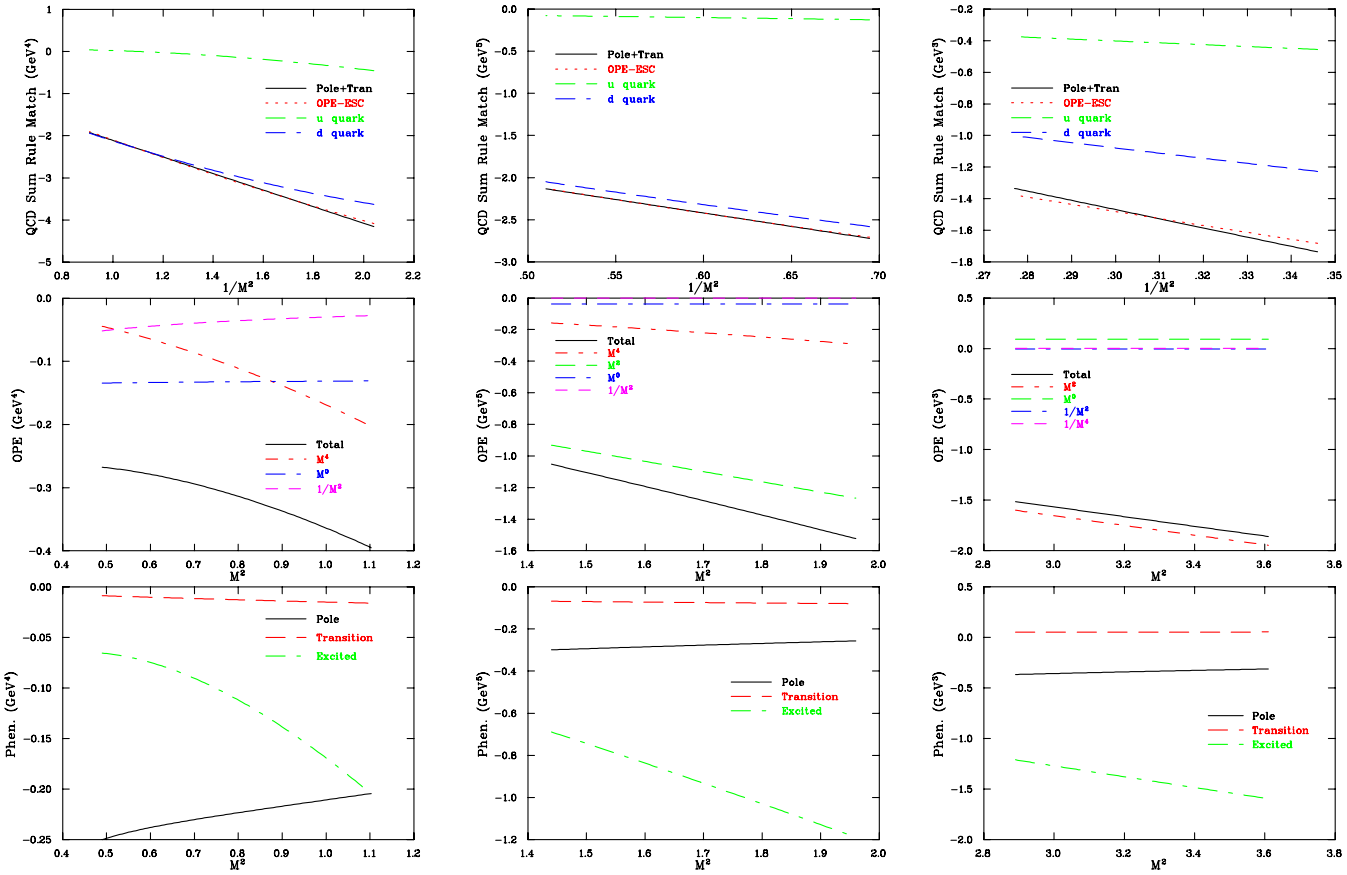

FIG. 8 (color online). Similar to Fig. 5, but for the neutron at all three structures: WE_1 (left panels), WE_1 (middle panels), WE_1 (right panels).

the small difference in the denominator $\Xi^- - \Xi^0$ which magnifies the apparent discrepancy. So this is not a good way of testing baryon independence. Our determination of the ratio of the left-hand side over the right-hand side (LHS/RHS) is 7.4(1.0), compared to the experimental value of 5.7(4) and the lattice calculation of 4.1(1.5). The errors are added in quadrature in forming these ratios.

One interesting sum rule [26] which is fairly accurately satisfied is

$$p + n = 3\Lambda + \tfrac{1}{2}(\Sigma^+ + \Sigma^-) - (\Xi^0 + \Xi^-). \tag{60}$$

It is derived using SU(3)-flavor symmetry to characterize the Λ wave function. Our determination of the LHS/RHS ratio is 1.24(79), compared to the experimental values of 1.22(5) and the lattice calculation of 1.45(27).

Another sum rule, first derived by Franklin [25],

$$p - n = \Sigma^+ - \Sigma^- + \Xi^- - \Xi^0, \tag{61}$$

is another test of baryon independence of the quark moments. The strange quarks approximately cancel, leaving only u and d quarks. We give the ratio of 1.20(0.68), while the experimental measurements give 1.133(10) and the lattice results are 1.07(8) for this ratio.

Finally, the Sachs sum rule [27]

$$3(p + n) = \Sigma^+ - \Sigma^- - \Xi^- + \Xi^0 \tag{62}$$

is satisfied by the more general extension of SU(6) symmetry and is another test of baryon independence of quark moments. This sum rule is just the sum of the two separate sum rules proposed earlier by Franklin [28]. Our result gives the ratio of 0.86(35) which is in agreement with the experimental measurements of 0.881(11). Whereas it yields an opposite violation with a ratio of 1.29(20) from lattice moments. This contradiction is possibly because the Sachs sum rule may be sensitive to dynamics not included in the lattice calculation.

E. Individual quark contributions

To gain a deeper understanding of the dynamics, it is useful to consider the individual quark sector contributions to the magnetic moment. In our approach, we can easily dial individual quark contributions to the QCD sum rules. For example, to turn off all u-quark contributions, we set the charge factor $e_u = 0$. To turn off all s-quark contributions, we set $e_s = 0$, $m_s = 0$, $f = 1$, and $\phi = 1$. We can extract a number corresponding to each quark contribution from the slope of Eq. (52) as a function of $1/M^2$. We call

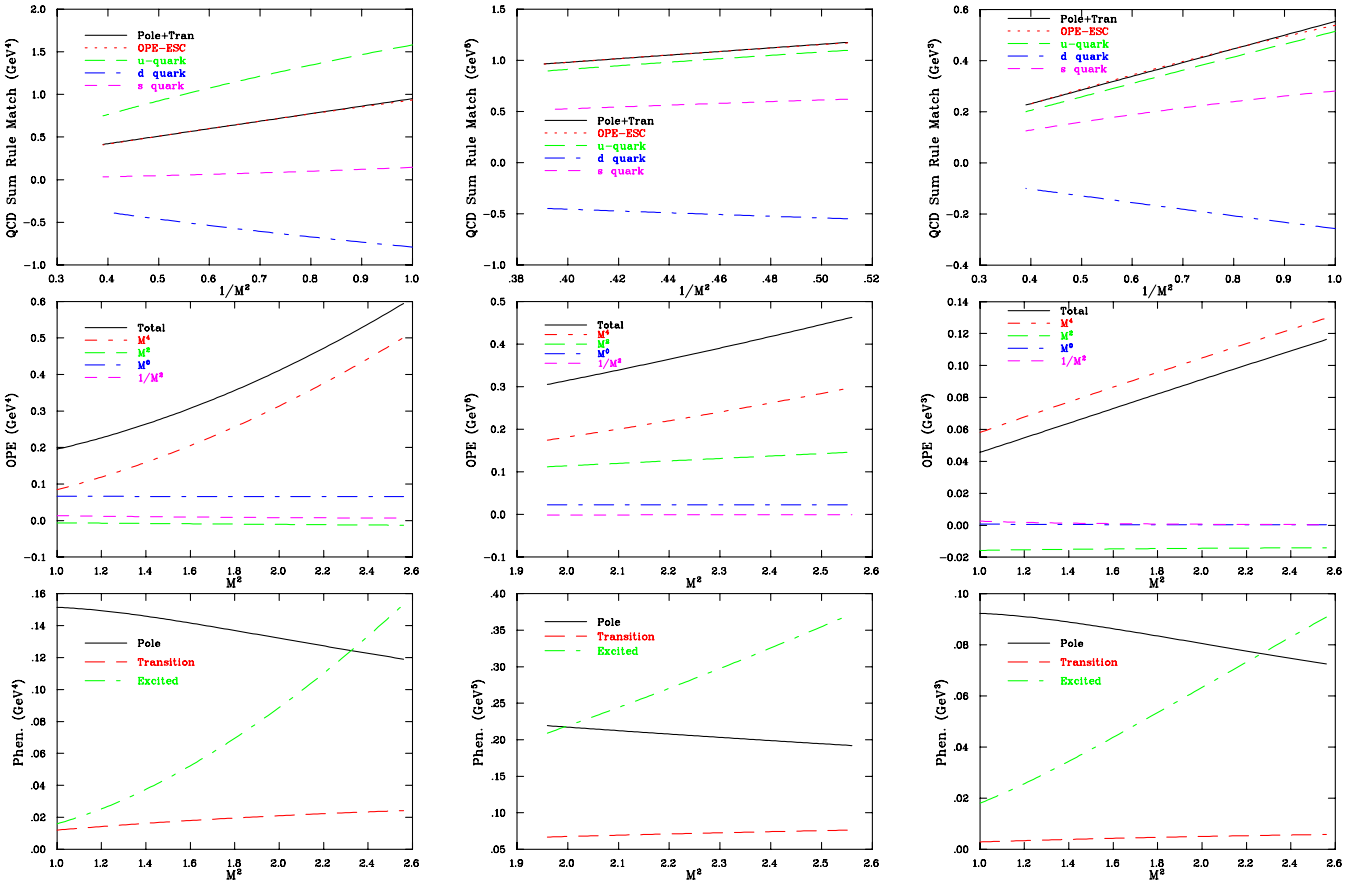

FIG. 9 (color online). Similar to Fig. 8, but for Σ^0.

this the raw individual quark contributions to the magnetic moments.

Table V gives the result of raw individual u, d, and s quark sector contributions to the magnetic moments from the QCD sum rules at WE_1. It is compared with the lattice QCD result in [23]. The lattice results were rescaled later in [29] and we use the rescaled results for the comparison. Our results agree with the lattice results reasonably well. The biggest discrepancy is that our light quark moments in Ξ^0 and Ξ^- are small. In Σ^0 and Λ, the total of u and d quark moments agrees very well with lattice data for light quark moments. Note that only a combined number for light quark ($\mu_l = \mu_u + \mu_d$) was given on the lattice [23]. To compare with our separated u and d quark numbers, we break up the lattice number by using the relation $\mu_u = -2\mu_d$.

In the simple quark model [30], the magnetic moment of the proton is given by $p = \frac{4}{3}\mu_u - \frac{1}{3}\mu_d$. In the SU(2) limit, there is the relation $\mu_u = -2\mu_d$. Our results for Σ^0 and Λ, the two uds structure baryons, agree with this very well. This relation also suggests that the ratio of the u quark and d quark contributions in proton is $\frac{4}{3}\mu_u/(-\frac{3}{4}\mu_d) = 8$. Our QCD sum rule ratio is 10.6 for $\beta = -1.2$, which agrees with the lattice ratio of 10.3(7) at κ_1. For the neutron the quark model ratio is $\frac{4}{3}\mu_d/(-\frac{1}{3}\mu_u) = 2$, and our result is 3.64(40) for this ratio, which differs from the SU(6) spin-flavor symmetry prediction. The lattice ratio is 2.6. The bigger ratio represents an enhancement of the doubly

TABLE IV. A comparison of selected ratios of magnetic moments.

Ratio	Sum rule result	SU(6) symmetry	Lattice results	Exp.
n/p	−0.70(9)	−2/3	−0.63(5)	−0.68
Σ^-/Σ^+	−0.50(7)	−1/3	−0.37(3)	−0.47
Ξ^-/Ξ^0	0.56(6)	1/2	0.58(5)	0.52
Ξ^0/Λ	2.05(56)	2	2.4(5)	2.04
Ξ^-/Λ	1.14(32)	1	1.0(2)	1.13

TABLE V. Individual quark contributions and total magnetic moments in units of nuclear magnetons extracted from the QCD sum rules at WE_1 (denoted by the subscript SR) are compared with those from a lattice QCD calculation (denoted by the subscript LAT) [23,29].

	$\mu^u_{\rm SR}$	$\mu^u_{\rm LAT}$	$\mu^d_{\rm SR}$	$\mu^d_{\rm LAT}$	$\mu^s_{\rm SR}$	$\mu^s_{\rm LAT}$	$\mu^{\rm Total}_{\rm SR}$	$\mu^{\rm Total}_{\rm LAT}$
p	2.46(25)	2.59(24)	0.38(4)	0.15(9)	0	0	2.82(26)	2.79
n	−0.42(9)	−0.31(20)	−1.53(13)	−1.32(14)	0	0	−1.97(15)	−1.60(21)
Λ	0.18(7)	0.09(6)	−0.09(4)	−0.03(2)	−0.63(15)	−0.54(7)	−0.56(15)	−0.50(7)
Σ^+	2.06(25)	2.33(29)	0	0	0.15(2)	0.08(5)	2.31(25)	2.37(18)
Σ^0	1.09(12)	0.87(9)	−0.54(6)	−0.29(3)	0.14(2)	0.08(5)	0.69(7)	0.65(6)
Σ^-	0	0	−1.25(10)	−1.14(14)	0.10(2)	0.08(5)	−1.16(10)	−1.08(10)
Ξ^0	0.02(2)	−0.44(6)	0	0	−1.08(7)	−0.73(6)	−1.15(5)	−1.17(9)
Ξ^-	0	0	0.03(2)	0.22(3)	−0.67(6)	−0.73(6)	−0.64(6)	−0.51(7)

represented quark contribution. These results suggest that although the total magnetic moments ratios agree with SU(6) ratios (see Table IV), the underlying quark dynamics are really quite different from different individual quark contributions.

To include the possible nonstatic effect, Franklin [26] proposed a generalization of SU(6) results so that nonstatic components are the same for each octet baryon:

$$\begin{aligned} p &= \tfrac{4}{3}\mu_u - \tfrac{1}{3}\mu'_d, \qquad n = \tfrac{4}{3}\mu_d - \tfrac{1}{3}\mu'_u, \\ \Sigma^+ &= \tfrac{4}{3}\mu_u - \tfrac{1}{3}\mu'_s, \qquad \Sigma^- = \tfrac{4}{3}\mu_d - \tfrac{1}{3}\mu'_s, \\ \Xi^0 &= \tfrac{4}{3}\mu_s - \tfrac{1}{3}\mu'_u, \qquad \Xi^- = \tfrac{4}{3}\mu_s - \tfrac{1}{3}\mu'_d, \\ \Sigma^0 &= \tfrac{2}{3}\mu_u + \tfrac{2}{3}\mu_d - \tfrac{1}{3}\mu'_s, \qquad \Lambda = \mu''_s, \end{aligned} \tag{63}$$

where quark symbols refer to quark moment contributions including nonstatic effect. The magnetic moment contribution of the unlike quark in the baryon is primed.

In order to compare with the effective quark moments defined in the quark model, we convert our raw quark moments in Table V quark in a similar fashion. Take the proton, for example, we define effective quark moments μ_u and μ'_d from QCD sum rules by $u_{\rm SR} = \frac{4}{3}\mu_u$, $d_{\rm SR} = \frac{1}{3}\mu'_d$. One can define effective moments for quarks in other baryons in a similar manner.

In the proton, μ_u is 1.84(18) while in Σ^+ 1.54(18), and in Σ^0 is 1.63(18). The magnetic moments listed here are all in units of μ_N. In the neutron, μ'_u is 1.25(27), which is smaller than μ_u. This is an example that the effective quark magnetic moment is sensitive to the environment the quark resides in. We find the following relation from our results:

$$\mu^p_u < \mu^{\Sigma^0}_u < \mu^{\Sigma^+}_u. \tag{64}$$

For μ_d, in n it is −1.15(11), while for Σ^0 it is −0.82(8), and for Σ^- it is −0.93(8). From p we can get $\mu'_d = -1.15(12)$. It has a similar relation for the absolute value

$$\mu^n_d < \mu^{\Sigma^0}_d < \mu^{\Sigma^-}_d. \tag{65}$$

For μ_s, it is −0.81(6) in Ξ^0 and −0.50(5) in Ξ^-. For μ'_s, it is −0.45(5), −0.42(5) and −0.30(5) in Σ^+, Σ^0, and Σ^-, respectively. From Λ we can get μ''_s about −0.63(15).

For these individual quark effective moments, we notice that in general we have the following relation:

$$\mu_s < \mu_d < \mu_u. \tag{66}$$

It is expected because of the quark mass effects, which is analogous to those seen in the electric properties.

Another way of looking at the individual effective quark moments is by expressing them in terms of baryon magnetic moments using Eq. (63) and isospin symmetry. For example, the d-quark effective moment can be expressed as

$$\mu_d = -\tfrac{1}{4}(2p + n) = \tfrac{1}{4}(\Sigma^- - \Sigma^+). \tag{67}$$

Our result indicates $\mu_d = -0.92(14) < -0.86(7)$ using the baryon moments in Table V or in Table I. It agrees well with the experimental moments $\mu_d = -0.918 < -0.894(7)$ and the lattice result of $\mu_d = -1.00(5) < -0.86(6)$.

Similarly the d' quark effective moment is

$$\mu'_d = p + 2n = \Xi^0 - \Xi^-. \tag{68}$$

We have $\mu'_d = -1.12(39) < -0.51(8)$. It also agrees very well with the experimental moments $\mu'_d = -1.003 < -0.578(26)$ although the two sides of this sum do not agree well.

The strange quark can be isolated as

$$\begin{aligned} &\mu_s = \frac{1}{4}(\Xi^0 + 2\Xi^-), \qquad \mu'_s = -\Sigma^+ - 2\Sigma^-, \\ &\mu''_s = \Lambda - \delta. \end{aligned} \tag{69}$$

Our results are compared with experiment and lattice calculation in Table VI. Not only do the results agree with the experiment and lattice calculation, they also roughly agree with the strange quark moments from individual quark moments.

Now, we can look at the quark moment difference such as $\mu'_s - \mu'_d$ and $\mu_s - \mu_d$. According to a simple quark model, the difference should be the same and approximately as 0.36. In fact, from

TABLE VI. The results for s s', and s'' quark effective moments from QCD sum rule, experiment, and lattice calculation.

	μ_s	μ_s''	μ_s'
SR	$-0.61(3)$	$<-0.60(15)$	$<0.01(32)$
Exp.	$-0.651(12)$	$<-0.57(4)$	$<-0.107(36)$
LAT.	$-0.55(4)$	$\approx -0.54(4)$	$<-0.24(17)$

$$\mu_s' - \mu_d' = 3(p - \Sigma^+), \tag{70}$$

$$\mu_s - \mu_d = \frac{3}{4}(\Xi^0 - n), \tag{71}$$

QCD sum rules give 1.53(8) and 0.61(12). The experiment gives 1.12(7) and 0.495(11), while lattice calculation gives 1.3(5) and 0.32(17), respectively. The large result of $\mu_s' - \mu_d'$ is difficult to reconcile with any simple model. And Eq. (70) is a poor way to measure the difference of s and d quark contributions.

F. Correlations

Our Monte Carlo analysis affords the opportunity to study the correlations between any two parameters since the entire QCD input phase space is mapped into the phenomenological output space. This correlation can be explored by a scatter plot of the two parameters of interest.

Figure 10 shows the scatter plots for the proton magnetic moment at structure WE_1. We see that the magnetic moment has a strong correlation with the vacuum susceptibility χ. It is a negative correlation meaning larger χ (in absolute terms since χ is negative) leads to smaller μ_B. A slight negative correlation with the mixed condensate and a slight positive correlation with another vacuum susceptibility κ are also observed. Precise determination of the QCD parameters, especially for those that have strong correlations to the output parameters, is crucial for keeping the uncertainties in the spectral parameters under control.

Figure 11 shows a similar plot for the Σ^0 at structure WE_1. Here we focus on the three vacuum susceptibilities and the three parameters that define the strange quark (m_s, f, and ϕ). The correlations with the other condensates are

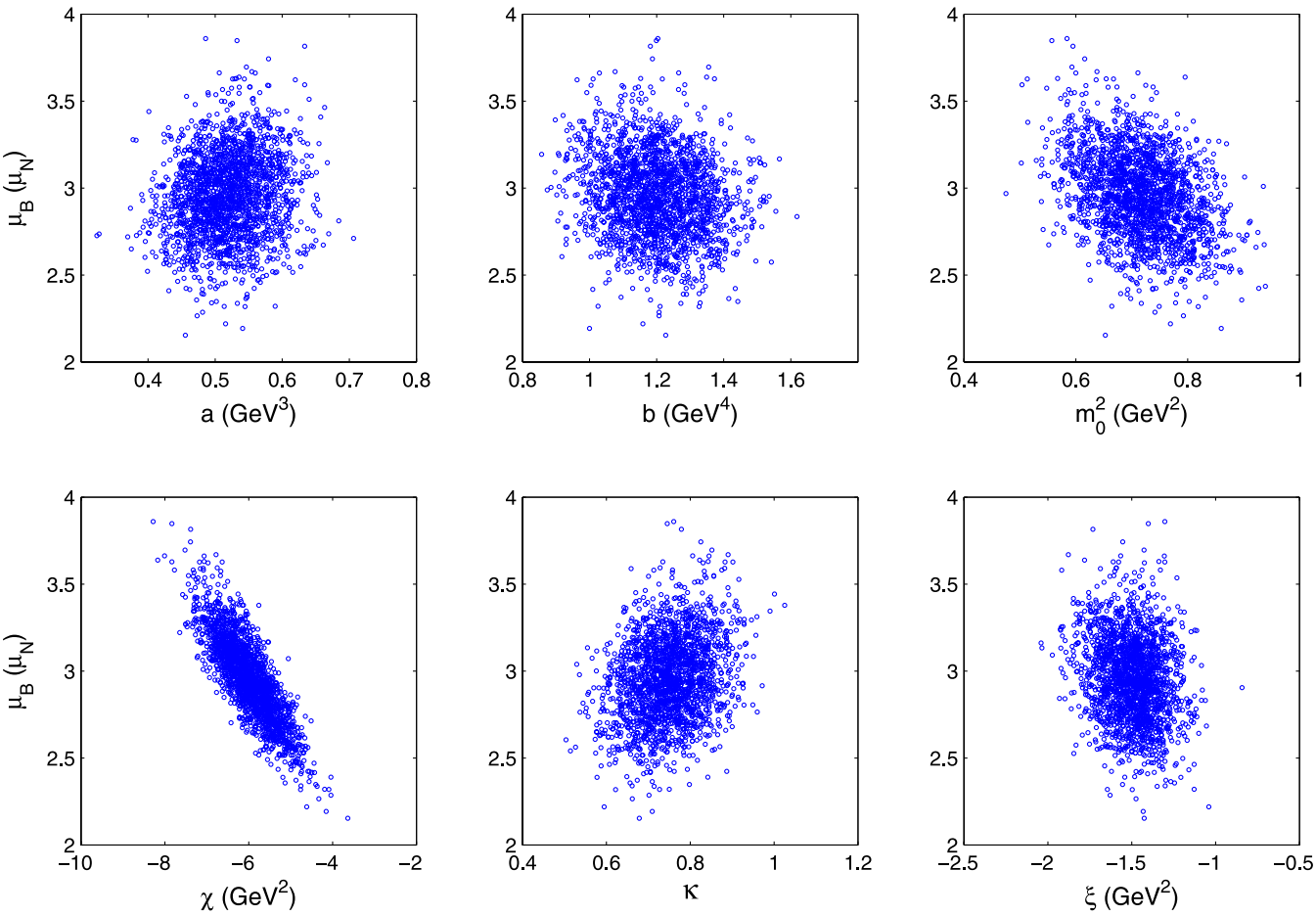

FIG. 10 (color online). Scatter plots showing correlations between the magnetic moment and the QCD parameters for the proton at structure WE_1. They are obtained from 2000 Monte Carlo samples with 10% uncertainty on all the QCD parameters.

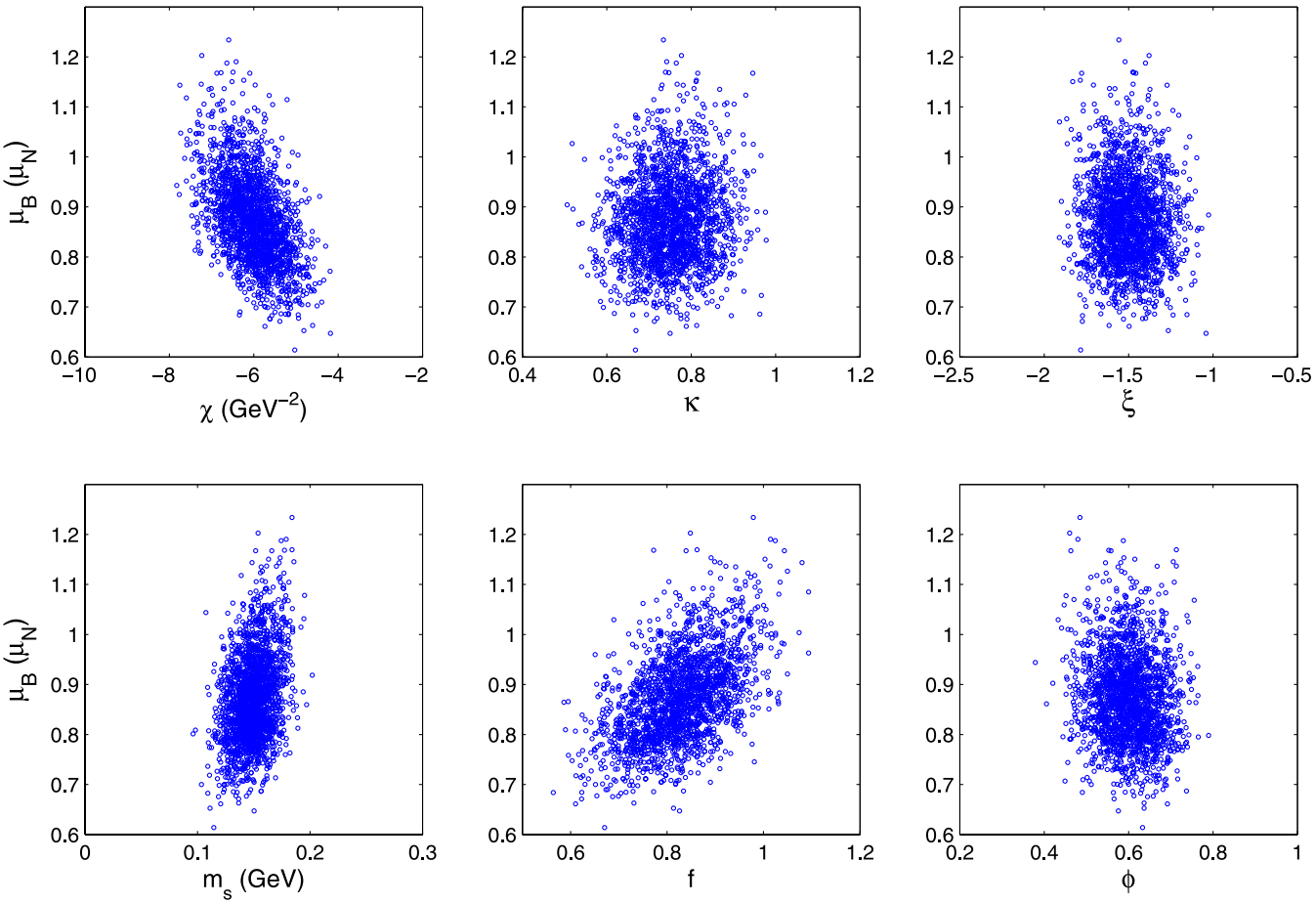

FIG. 11 (color online). Similar to Fig. 10, but for the Σ^0 and a different set of QCD parameters.

similar to the proton and are not shown. A negative correlation with χ exists, but not as strong as that for the proton. A slight positive correlation with m_s and f is also observed.

VI. CONCLUSION

We have carried out a comprehensive study of the magnetic moment of octet baryons using the method of QCD sum rules. We derived a new, complete set of QCD sum rules using generalized interpolating fields and examined them by a Monte Carlo analysis. Here is a summary of our findings.

We proposed a new way of determining the magnetic moments from the slope of straight lines. We find this method more robust than from the normalization (intercept) or from looking for "flatness" as a function of Borel mass. The linearity displayed from the OPE side matches almost perfectly with the phenomenological side in most cases. The method also demonstrates clearly that the transition terms caused by the external field in the intermediate terms cannot be ignored. They are needed to make the two sides of a QCD sum rule match.

Out of the three independent structures, we find that the sum rules from the WE_1 structure are the most reliable based on OPE convergence and ground-state pole dominance. The QCD sum rules from this structure are in Eq. (32); its predictions are found in Table I, and convergence properties are displayed in Fig. 5. They should be considered as the best results in this work. The extracted magnetic moments are in good agreement with experiment. These results are used to shed light on a variety of magnetic moment sum rules based on SU(6) spin-flavor symmetries in the quark model, along with experiment and lattice QCD. Reasonable results from the other two structures (WO_1 and WO_2) are obtained for the first time, but they are less reliable due to poor convergence properties.

Our Monte Carlo analysis revealed that there is an uncertainty on the level of 10% in the magnetic moments if we assign 10% uncertainty in the QCD input parameters. It goes up to about 30% if we adopt the conservative assignments that have a wide range of uncertainties in Ref. [20]. The Monte Carlo analysis also revealed some correlations between the input and output parameters. The most sensitive is the vacuum susceptibility χ. So a better determination of this parameter can help improve the accuracy on the magnetic moments and other quantities computed from the same method.

We also isolated the individual quark contributions to the magnetic moments. These contributions provide insight into the rich dynamics in the baryons. By comparing them with the simple quark model and lattice QCD results, we reveal the effects of SU(3)-flavor symmetry breakings in the strange quark, the environment sensitivity of quarks in different baryons.

Taken together, this work can be considered an updated and improved determination of the magnetic moments of octet baryons, bringing it to the same level of sophistication as the decuplet baryons [9]. One possible extension along this line is a calculation of the N to Δ electromagnetic transition amplitudes which to our knowledge have not been studied in this method.

ACKNOWLEDGMENTS

This work is supported in part by the U.S. Department of Energy under Grant No. DE-FG02-95ER-40907.

[1] M. A. Shifman, A. I. Vainshtein, and Z. I. Zakharov, Nucl. Phys. **B147**, 385 (1979); **B147**, 448 (1979).
[2] I. I. Balitsky and A. V. Yung, Phys. Lett. **129B**, 328 (1983).
[3] B. L. Ioffe and A. V. Smilga, Nucl. Phys. **B232**, 109 (1984).
[4] B. L. Ioffe and A. V. Smilga, Phys. Lett. **133B**, 436 (1983).
[5] C. B. Chiu, J. Pasupathy, and S. L. Wilson, Phys. Rev. D **33**, 1961 (1986).
[6] J. Pasupathy, J. P. Singh, S. L. Wilson, and C. B. Chiu, Phys. Rev. D **36**, 1442 (1987).
[7] S. L. Wilson, J. Pasupathy, and C. B. Chiu, Phys. Rev. D **36**, 1451 (1987).
[8] S. Zhu, W. Hwang, and Z. Yang, Phys. Rev. D **57**, 1527 (1998).
[9] F. X. Lee, Phys. Rev. D **57**, 1801 (1998).
[10] F. X. Lee, Phys. Lett. B **419**, 14 (1998).
[11] J. Dey, M. Dey, and A. Iqubal, Phys. Lett. B **477**, 125 (2000).
[12] M. Sinha, A. Iqubal, M. Dey, and J. Dey, Phys. Lett. **562**, 63 (1998); , Phys. Lett. B **610**, 283 (2005).
[13] A. Samsonov, Phys. At. Nucl. **68**, 114 (2005).
[14] T. M. Aliev, I. Kanik, and M. Savci, Phys. Rev. D **68**, 056002 (2003).
[15] T. M. Aliev, A. Ozpineci, and M. Savci, Phys. Rev. D **66**, 016002 (2002).
[16] T. M. Aliev, A. Ozpineci, and M. Savci, Phys. Lett. B **516**, 299 (2001).
[17] T. M. Aliev, A. Ozpineci, and M. Savci, Nucl. Phys. **A678**, 443 (2000).
[18] B. L. Ioffe, Nucl. Phys. **B188**, 317 (1981); **191**, 591(E) (1981).
[19] A. Ozpineci, S. B. Yakovlev, and V. S. Zamiralov, Atom. Nucl. Phys. **68**, 304 (2005); Mod. Phys. Lett. A **20**, 243 (2005); and private communications.
[20] D. B. Leinweber, Ann. Phys. (N.Y.) **254**, 328 (1997).
[21] S. Coleman and S. Glashow, Phys. Rev. Lett. **6**, 423 (1961).
[22] F. X. Lee and X. Liu, Phys. Rev. D **66**, 014014 (2002).
[23] D. B. Leinweber, Phys. Rev. D **43**, 1659 (1991).
[24] H. J. Lipkin, Phys. Rev. D **24**, 1437 (1981).
[25] J. Franklin, Phys. Rev. **182**, 1607 (1969).
[26] J. Franklin, Phys. Rev. D **29**, 2648 (1984).
[27] R. G. Sachs, Phys. Rev. D **23**, 1148 (1981).
[28] J. Franklin, Phys. Rev. D **20**, 1742 (1979).
[29] D. B. Leinweber, Phys. Rev. D **45**, 252 (1992).
[30] D. H. Perkins, *Introduction to High Energy Physics* (Cambridge University Press, Cambridge, England, 2000), 4th ed.